



OPEN ACCESS

EDITED BY

Yuling Han,
Chinese Academy of Sciences (CAS), China

REVIEWED BY

Xiaolei Li,
University of Pennsylvania, United States
Vukasin M. Jovanovic,
National Center for Advancing Translational
Sciences (NIH), United States

*CORRESPONDENCE

Mari Spildrejorde,
✉ mari.spildrejorde@medisin.uio.no

†PRESENT ADDRESS

Magnus Leithaug,
Department of Analysis and Diagnostics,
Section for Molecular Biology, Norwegian
Veterinary Institute, Ås, Norway
Ankush Sharma,
Acerta Pharma (a member of AstraZeneca Plc),
Oss, Netherlands

†These authors have contributed equally to
this work

RECEIVED 06 May 2024

ACCEPTED 13 June 2024

PUBLISHED 11 July 2024

CITATION

Spildrejorde M, Leithaug M, Samara A,
Aass HCD, Sharma A, Acharya G, Nordeng H,
Gervin K and Lyle R (2024), Citalopram exposure
of hESCs during neuronal differentiation
identifies dysregulated genes involved in
neurodevelopment and depression.
Front. Cell Dev. Biol. 12:1428538.
doi: 10.3389/fcell.2024.1428538

COPYRIGHT

© 2024 Spildrejorde, Leithaug, Samara, Aass,
Sharma, Acharya, Nordeng, Gervin and Lyle.
This is an open-access article distributed under
the terms of the [Creative Commons Attribution
License \(CC BY\)](https://creativecommons.org/licenses/by/4.0/). The use, distribution or
reproduction in other forums is permitted,
provided the original author(s) and the
copyright owner(s) are credited and that the
original publication in this journal is cited, in
accordance with accepted academic practice.
No use, distribution or reproduction is
permitted which does not comply with these
terms.

Citalopram exposure of hESCs during neuronal differentiation identifies dysregulated genes involved in neurodevelopment and depression

Mari Spildrejorde^{1,2,3,4*}, Magnus Leithaug^{1,2†}, Athina Samara^{5,6,7},
Hans Christian D. Aass⁸, Ankush Sharma^{9,10,11†},
Ganesh Acharya^{12,13}, Hedvig Nordeng^{1,14}, Kristina Gervin^{1,4,14‡} and
Robert Lyle^{1,2,15‡}

¹PharmaTox Strategic Research Initiative, Faculty of Mathematics and Natural Sciences, University of Oslo, Oslo, Norway, ²Department of Medical Genetics, Oslo University Hospital and University of Oslo, Oslo, Norway, ³Institute of Clinical Medicine, Faculty of Medicine, University of Oslo, Oslo, Norway, ⁴Division of Clinical Neuroscience, Department of Research and Innovation, Oslo University Hospital, Oslo, Norway, ⁵Division of Clinical Paediatrics, Department of Women's and Children's Health, Karolinska Institutet, Solna, Sweden, ⁶Astrid Lindgren Children's Hospital, Karolinska University Hospital, Stockholm, Sweden, ⁷Department of Biomaterials, FUTURE Center for Functional Tissue Reconstruction, University of Oslo, Oslo, Norway, ⁸The Flow Cytometry Core Facility, Department of Medical Biochemistry, Oslo University Hospital, Ullevål, Oslo, Norway, ⁹Department of Cancer Immunology, Institute for Cancer Research, Oslo University Hospital, Oslo, Norway, ¹⁰KG Jebsen Centre for B-cell Malignancies, Institute of Clinical Medicine, University of Oslo, Oslo, Norway, ¹¹Precision Immunotherapy Alliance, University of Oslo, Oslo, Norway, ¹²Division of Obstetrics and Gynecology, Department of Clinical Science, Intervention and Technology (CLINTEC), Karolinska Institutet, Solna, Sweden, ¹³Center for Fetal Medicine, Karolinska University Hospital, Solna, Sweden, ¹⁴Pharmacoepidemiology and Drug Safety Research Group, Department of Pharmacy, University of Oslo, Oslo, Norway, ¹⁵Centre for Fertility and Health, Norwegian Institute of Public Health, Oslo, Norway

Selective serotonin reuptake inhibitors (SSRIs), including citalopram, are widely used antidepressants during pregnancy. However, the effects of prenatal exposure to citalopram on neurodevelopment remain poorly understood. We aimed to investigate the impact of citalopram exposure on early neuronal differentiation of human embryonic stem cells using a multi-omics approach. Citalopram induced time- and dose-dependent effects on gene expression and DNA methylation of genes involved in neurodevelopmental processes or linked to depression, such as *BDNF*, *GDF11*, *CCL2*, *STC1*, *DDIT4* and *GAD2*. Single-cell RNA-sequencing analysis revealed distinct clusters of stem cells, neuronal progenitors and neuroblasts, where exposure to citalopram subtly influenced progenitor subtypes. Pseudotemporal analysis showed enhanced neuronal differentiation. Our findings suggest that citalopram exposure during early neuronal differentiation influences gene expression patterns associated with neurodevelopment and depression, providing insights into its potential neurodevelopmental impact and highlighting the importance of further research to understand the long-term consequences of prenatal SSRI exposure.

KEYWORDS

citalopram, depression, epigenetics, neurodevelopment, human embryonic stem cells, single-cell RNA-seq, DNA methylation, multi-omics

1 Introduction

Depression and anxiety disorders have been associated with impaired serotonergic neurotransmission (Pollock, 2001). In the adult brain, serotonin regulates stress responses, cognition, attention, emotion, nociception, sleep and arousal (Brummelte et al., 2017). During fetal neurodevelopment, serotonin acts as a trophic factor and plays a crucial role in regulation of cell growth, differentiation, migration, myelination and synaptogenesis (Brummelte et al., 2017). Selective serotonin reuptake inhibitors (SSRIs) comprise a class of antidepressants that impede the reuptake of serotonin from the synaptic cleft of the pre-synaptic cell, thus restoring extracellular serotonin levels and increasing serotonergic neurotransmission (Sangkuhl et al., 2011). Consequently, there is the possibility that SSRI-exposure during early embryonic development could affect important neurodevelopmental pathways associated with serotonin signalling.

SSRIs are the first-choice class of antidepressants during pregnancy in many countries, and the reported use during pregnancy ranges from 1%–7% in European countries and 5%–8% in North America (Cooper et al., 2007; Mitchell et al., 2011; Jimenez-Solem et al., 2013; Charlton et al., 2015; Zoega et al., 2015). In Nordic countries, citalopram and its enantiomer escitalopram are among the most prescribed SSRIs to pregnant women (Nordeng et al., 2012; Charlton et al., 2015; Zoega et al., 2015). Some evidence of altered behaviour in offspring has been reported in rodent studies of early SSRI exposure (Ramsteijn and Olivier, 2020), whereas the effect on human development and, in particular, long-term neurodevelopmental outcomes is conflicting (Hjorth et al., 2019). While some epidemiological studies have indicated increased risk of depressive symptoms, social-behavioural disturbances (Klinger et al., 2011; Hanley et al., 2015; Malm et al., 2016; Lupattelli et al., 2018), Attention Deficit/Hyperactivity Disorder (ADHD) and Autism Spectrum Disorder (ASD) (Kobayashi et al., 2016; Andalib et al., 2017; Jiang et al., 2018; Morales et al., 2018), others have not (Jiang et al., 2018; Morales et al., 2018). Moreover, the methods and materials, as well as sample size and quality of these studies varies profoundly.

Environmental exposures during pregnancy may disrupt normal neurodevelopment and modulate the risk of neurodevelopmental disorders (NDDs) in the child. Epigenetic modifications, including DNA methylation (DNAm), have been proposed as mechanisms for this link (Kundakovic and Jaric, 2017). Epigenetic modifications are essential for cellular differentiation and fetal neurodevelopment. Prenatal exposures may impact these epigenetic modifications, inducing long-term adverse effects on brain structure and function (Kundakovic and Jaric, 2017). However, studies assessing the causal underlying mechanisms involved in prenatal exposure to SSRIs and increased risk of altered neurodevelopment are sparse. Recently, we identified epigenetic patterns (i.e., DNAm) in cord blood at birth from children exposed to maternal depression and (es)citalopram during pregnancy and neurodevelopmental trajectories in early childhood (Olstad et al., 2023).

SSRIs have previously been studied at therapeutic concentrations using *in vitro* neuronal differentiation models. In differentiating human hippocampal progenitors, exposure to sertraline for 10 days increased neuronal differentiation (Anacker et al., 2011). In human cortical spheroids, chronic exposure to

fluoxetine reversibly altered neuronal activity but did not induce changes to synapse formation (Tate et al., 2021). Further, in human iPSC-derived brain organoids, exposure to paroxetine for 8 weeks induced changes to neurite outgrowth, synaptic markers, myelination and cell composition (Zhong et al., 2020). However, to the best of our knowledge, there are no studies that investigate the effect of long-term exposure of citalopram to *in vitro* human neuronal differentiation.

In the present study, we aimed to identify the effect of citalopram exposure during early neurodevelopment using a recently published *in vitro* platform of neuronal differentiation of human embryonic stem cells (hESCs) towards telencephalic neurons, corresponding to first trimester human development (Samara et al., 2022a; 2022b). This model for studying the effects of maternal medication intake on early fetal brain development provides a unique opportunity to study the effect on gene expression and DNAm in otherwise inaccessible window of development. We focused specifically on citalopram exposure during early pregnancy as this is considered a susceptible period for neurotoxicity, i.e., the foundation of neurodevelopment is laid in the first trimester (Moore et al., 2016). This is the time period with highest prevalence of antidepressant use in pregnancy (Nordeng et al., 2012; Zoega et al., 2015), when many women could be unaware of their pregnancy status. A multi-omics approach with single-cell RNA sequencing (scRNAseq), bulk RNAseq and DNAm was used to investigate citalopram time- and dose-specific effects on gene expression and DNAm during early neuronal differentiation, assessing the potential molecular neurodevelopmental effects of citalopram.

2 Materials and methods

Critical reagents and resources are displayed in Supplementary Table S1. All original code can be found at https://github.com/maspil/Citalopram_multiomics.

2.1 hESC maintenance

Human embryonic stem cells HS360 (Karolinska Institutet, Sweden, RRID:CVCL_C202) (Ström et al., 2010; Main et al., 2020) were cultured as previously described (Samara et al., 2022a). Briefly, cells were maintained in Essential eight medium (E8, ThermoFisher) on Geltrex (ThermoFisher) pre-coated 6-well culture plates.

2.2 Neuronal differentiation of hESCs and exposure to citalopram

To study the *in vitro* effects of citalopram, HS360 hESCs cells were differentiated according to Samara and Spildrejorde et al., 2023; Samara et al., 2022a) with minor changes. Briefly, 70,000 cells/well were seeded in Geltrex pre-coated 12-well plates at Day 0. During Days 1–13, media was changed daily: cells were exposed to media only (control) or media containing citalopram (Sigma-Aldrich). The therapeutic concentration range of citalopram in plasma is considered to be 150–340 nM (Hiemke et al., 2018),

however lower concentrations have been measured in cord blood (Hendrick et al., 2003; Rampono et al., 2009; Paulzen et al., 2017). Thus, to cover concentrations relevant for the *in vivo* situation, cells were exposed to 50, 100, 200 or 400 nM citalopram. Neural induction started at Day 1 using base medium (Advanced DMEM/F12 (ThermoFisher), 1% GlutaMAX (GIBCO), 1% Penicillin/Streptomycin (ThermoFisher), 1% N2 supplement (ThermoFisher)) containing 10 μ M SB431542 (Sigma-Aldrich), 100 nM LDN-193189 (STEMCELL Technologies) and 2 μ M XAV939 (STEMCELL Technologies). At Day 7, cells were seeded at 525,000 cells/well on 12-well culture plates sequentially coated with polyornithine (Sigma-Aldrich), fibronectin (ThermoFisher) and Geltrex, using base medium containing 1% B27 supplement through till Day 13. Cells were harvested for downstream analysis at Day 0, 6, 10 and 13.

2.3 Cell viability assay

HS360 cells were washed twice with PBS and collected using Accutase (STEMCELL technologies) and seeded at 20,000 cells/well in Geltrex-coated 96-well plates and incubated in E8 containing 10 μ M Rock inhibitor (Y-27632, STEMCELL technologies) at 37°C/5% CO₂ for 24 h. Media was then changed to E8 alone (control) or E8 containing 0.025, 0.05, 0.1, 0.2, 0.4, 0.8, 3.2, 12.8, 51.2 or 204.8 μ M citalopram (Sigma-Aldrich) in quintuplicate wells. Cells were incubated for 24 h at 37°C/5% CO₂ and cell viability was assessed using CellTiter-Glo[®] Luminescent Cell Viability Assay (Promega) according to manufacturer's instructions.

2.4 Flow cytometry

HS360 cells (Day 0) and cells differentiated to Day 13 were washed twice with PBS, collected using Accutase and resuspended in wash medium (Day 0: E8, Day 13: Ad. DMEM). Cells were then centrifuged (300 x g for 4 min), supernatants were removed and washed in PBS (300 x g for 4 min). Cells used with intracellular markers against SOX1, β 3-Tubulin and OCT4, were fixed as follows: Supernatants were removed, cells were resuspended in 1 mL/1 \times 10⁷ cells Cytotfix Fixation Buffer (BD Biosciences) and incubated for 20 min at room temperature (RT) in the dark. To permeabilize the cell membranes, cells were washed twice (300 x g for 4 min) with 1 mL/1 \times 10⁷ cells 1X Perm/Wash buffer (BD Biosciences). Cells were then resuspended in 1X Perm/Wash buffer and incubated for 10 min at RT. To block and stain cells, a total volume of 100 μ L of cells, antibodies and 1X Perm/Wash buffer were incubated for 30 min in the dark according to concentrations found in [Supplementary Table S2](#). Following incubation, cells were washed twice (300 x g for 4 min) in 1 mL 1X Perm/Wash buffer and resuspended in Stain Buffer (FBS) (BD Biosciences) to a concentration of 1-3 \times 10⁶ cells/mL and data was acquired by flow cytometry using Accuri C6 (Becton Dickinson, San Jose, CA, United States). Raw data was analysed using FlowJo software v.10. Delta median fluorescence intensity (Δ MFI) of gated populations of live/singlets cells was calculated by subtracting the MFI of corresponding isotype control to the MFI of antibody of interest (n = 3). Results were visualized using R software (R Core

Team, 2021) and the Tidyverse R package v.1.3.1 (Wickham et al., 2019).

2.5 DNA/RNA purification

Cells were washed with PBS and collected by direct lysis in the cell culture well. Genomic DNA and total RNA were isolated from the same biological sample using RNA/DNA purification kit (Norgen Biotek Corp.) and RNA was purified using on-column RNase-Free DNase I Kit (Norgen Biotek Corp.). Nucleic acid quantification was performed using Qubit (ThermoFisher Scientific), purity was measured using Nanodrop 2000 (ThermoFisher Scientific), while RNA and DNA integrity was assessed using 2,100 Bioanalyzer (Agilent Technologies) and 4,200 TapeStation (Agilent Technologies), respectively.

2.6 Bulk transcriptome sequencing

The sequencing libraries were prepared with TruSeq Stranded mRNA Library Prep (Illumina, San Diego, CA) according to manufacturer's instructions. The 89 libraries ([Supplementary Table S3](#)) were pooled at equimolar concentrations and sequenced on a NovaSeq 6000 S4 flow cell with 150 bp paired end reads (Illumina, San Diego, CA). The quality of sequencing reads was assessed using BBMap v.34.56 (Bushnell, 2014), and adapter sequences and low-quality reads were removed. The sequencing reads were then mapped to the GRCh38 index using HISAT2 v.2.1.0 (Kim et al., 2015). Mapped paired end reads were counted to features using featureCounts v.1.4.6 (Liao et al., 2014). Differential expression (DE) analysis was conducted in R (R Core Team, 2021) using glmQLFTest function in edgeR v.3.34.1 (Robinson et al., 2010; Zhou et al., 2014; Lun et al., 2016). Benjamini-Hochberg was used to correct for multiple testing and genes were considered significantly differentially expressed with an FDR <0.01 and <0.05 for control ([Supplementary Figures S2, S3](#)) and citalopram comparisons, respectively. The linear time-response analysis was conducted using the following model: $\sim 0 + \text{Day} * \text{Concentration}$, where Day was classified as numeric and Concentration was classified as factors. The non-linear time-response analysis was conducted using the following model: $\sim 0 + \text{Concentration} * X$, where X was the B-spline basis matrix for a natural cubic spline using Day as predictor variable and degrees of freedom = 2. The linear dose-response analysis was conducted using the following model: $\sim 0 + \text{Day} * \text{Concentration}$, where Day was classified as factors and Concentration was classified as numeric. The non-linear dose-response analysis was conducted using the following model: $\sim 0 + \text{Day} * X$, where X was the B-spline basis matrix for a natural cubic spline using Concentration as predictor variable and degrees of freedom = 3. Normalized counts were visualized using the Tidyverse package v.1.3.1 (Wickham et al., 2019). The heatmaps were generated using Pheatmap package v.1.0.12 (Kolde, 2019). The gene set enrichment analysis (GSEA) of pre-ranked gene lists, based on *p*-values and direction of expression change, were performed using GSEA software

(Subramanian et al., 2005) identifying biological processes (BP) terms. The size of the analysed gene sets was restricted to 20–1,000 genes, and the chip annotation used was “Human_ENSEMBL_Gene_ID_MSigDB.v7.4. chip”.

2.7 DNA methylation analysis

DNA_m status of 89 samples (Supplementary Table S3) were assessed using the Infinium MethylationEPIC BeadChip v.1.0_B3 (Illumina, San Diego, CA). Quality control and pre-processing of the raw data was performed in R (R Core Team, 2021) using Minfi v.1.38.0 (Aryee et al., 2014). No samples were removed due to poor quality (detection *p*-values >0.05). Background correction was performed using NOOB method (Triche et al., 2013) and β values (ratio of methylated signal divided by the sum of the methylated and unmethylated signal) were normalized using functional normalization (Fortin et al., 2014). Probes with unreliable measurements (detection *p*-values >0.01) (*n* = 11,740) and cross-reactive probes (Chen et al., 2013) (*n* = 43,256) were then removed, resulting in a final data set consisting of 811,233 probes and 89 samples. Probes were annotated with Illumina Human Methylation EPIC annotation 1.0 B5 (hg38). Differential methylation (DM) analysis was performed on the *M* values (log₂ of the β values) using the limma package v.3.48.3 (Ritchie et al., 2015). The linear time-response analysis was conducted using the following model: $\sim 0 + \text{Day} * \text{Concentration}$, where Day was classified as numeric and Concentration was classified as factors. The non-linear time-response analysis was conducted using the following model: $\sim 0 + \text{Concentration} * X$, where *X* was the B-spline basis matrix for a natural cubic spline using Day as predictor variable and degrees of freedom = 2. The dose-response analysis was conducted using the following model: $\sim 0 + \text{Day} * \text{Concentration}$, where Day was classified as factors and Concentration was classified as numeric. The non-linear dose-response analysis was conducted using the following model: $\sim 0 + \text{Day} * X$, where *X* was the B-spline basis matrix for a natural cubic spline using Concentration as predictor variable and degrees of freedom = 3. Benjamini–Hochberg was used to correct for multiple testing using and CpGs were considered significantly differentially methylated with an FDR <0.01 and <0.05 for control (Supplementary Figures S2, S3) and citalopram comparisons, respectively. Gene ontology analysis was performed using top 10,000 DMCs as input to gometh in the missMethyl package v.1.26.0 (Phipson et al., 2016) looking at BP terms.

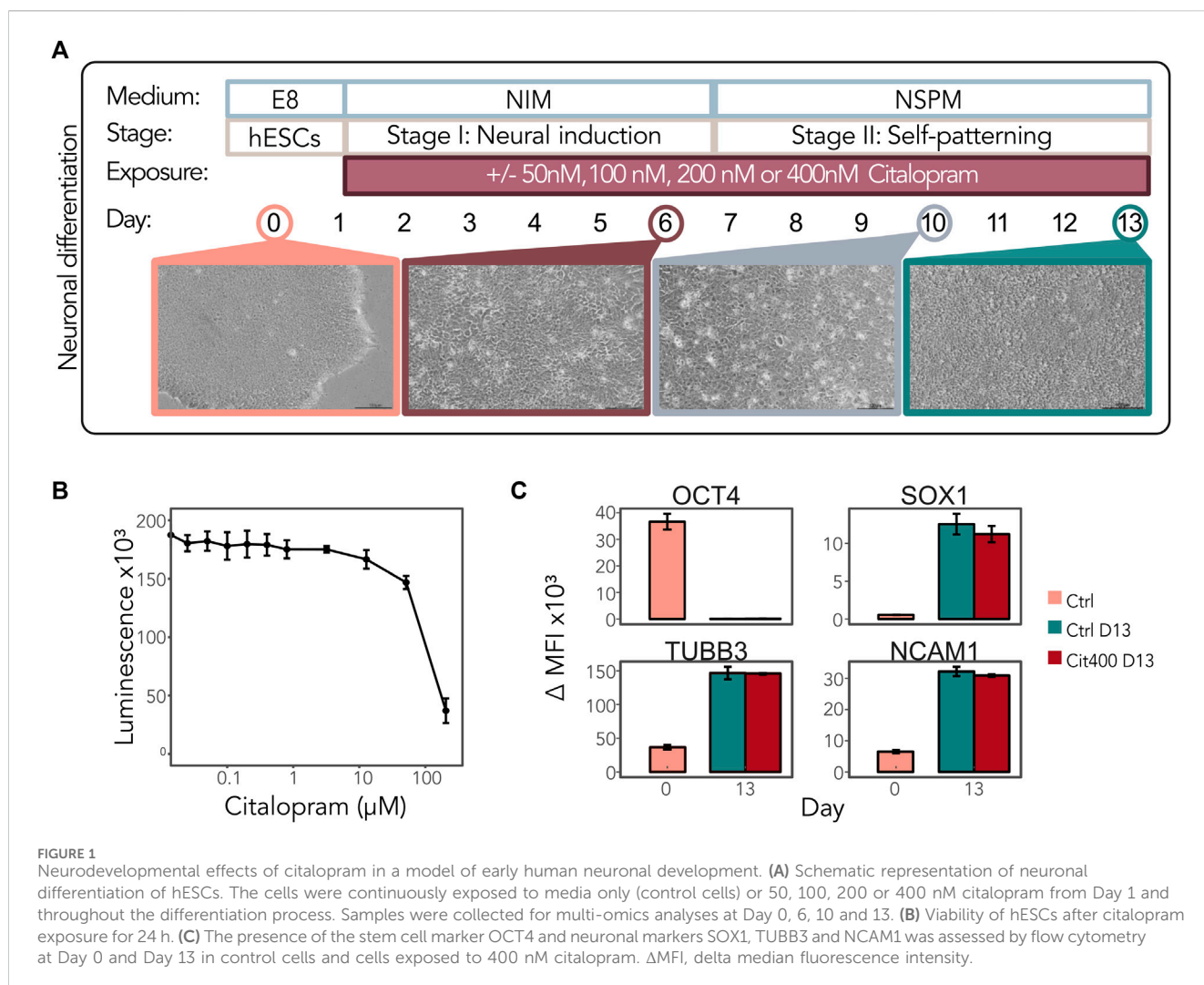
2.8 Collection of cells and single-cell RNA-sequencing

HS360 cells (Day 0) and cells at Day 6, 10 and 13 were washed twice in wells with PBS and detached using Accutase at 37°C for 7–10 min. Cells were then pipetted 10–15 times to separate into single cells and transferred to centrifuge tubes containing the appropriate base media (Day 0: E8, Day 6–13: Ad. DMEM) with 0.04% BSA (Sigma-Aldrich). Cell suspensions were counted and centrifuged at 300 × *g* for 5 min and the supernatant was discarded. Cell pellets were then resuspended in base media containing 0.04%

BSA and cell aggregates were filtered out using MACS SmartStrainers (Miltenyi). The cells were counted again and processed within 1 h on the 10x Chromium controller (10x Genomics) according to 10x Genomics protocol CG000315 (Rev A). Approximately 4,200 cells were loaded per channel on the Chromium Next GEM Chip G (10x Genomics) to give an estimated recovery of 2,500 cells. The Chromium Next GEM Single Cell 3' Kit v3.1 (10x Genomics) and Dual Index Kit TT Set A (10x Genomics) were used to generate single-cell (sc)RNA-seq libraries according to the manufacturer's instructions. Libraries from 16 samples were pooled together at equimolar concentrations and sequenced on a NovaSeq 6000 S1 flow cell (Illumina) with 28 cycles for read 1, 10 cycles for the I7 index, 10 cycles for the I5 index and 90 cycles for read 2.

2.9 scRNAseq analysis

The Cell Ranger 4.0.0 Gene Expression pipeline (10x Genomics) was used to demultiplex the raw base-call files and convert them into FASTQ files. The FASTQ files were aligned to the GRCh38 human reference genome (2020-A), and the Cell Ranger count quantified single-cell gene expression using default parameters. Cell Ranger's estimated number of recovered cells/sample were from 1,113–2,528, with mean reads/cell spanning from 27,000–119 000. Downstream analysis was performed using the R software (R Core Team, 2021). Duplicates, dead cells and cells with greater than five median absolute deviations (MADs) for mitochondrial reads were filtered out using the scater R package (McCarthy et al., 2017) resulting in a total of 20,217 cells (Supplementary Table S3) for downstream analysis. SCTransform with regression of cell cycle genes and mitochondrial content (Tirosh et al., 2016; Hafemeister and Satija, 2019) was used to normalise data. A resolution of 0.55 was used to cluster cells, obtained by determining the optimum number of clusters (cell grouped together sharing similar expression profiles) in the dataset using the Clustree R package (Zappia and Oshlack, 2018). Principal component analysis was performed using the RunPCA function, followed by FindClusters and RunUMAP functions of Seurat package (Stuart et al., 2019) to perform SNN-based UMAP clustering. The SingleR R package (Aran et al., 2019) was used to annotate the cells against a merged reference dataset derived from 1: from a Human Brain dataset (LaManno et al., 2016) and 2: a forebrain organoid dataset (Bhaduri et al., 2020), from the scRNAseq R package. Cell types with <10 cells annotated are excluded from the plots (Figures 5D, E). Slingshot R package was used to create the pseudotime differentiation trajectory (Street et al., 2018). Temporally expressed genes were identified by fitting generalized additive model for each gene using the gam R package (Hastie, 2022) and visualized using pheatmap (Kolde, 2019) and scater (McCarthy et al., 2017) R packages. Differential pseudotime analysis were calculated by removing Day 0 from dataset and looking at differences in pseudotime values between citalopram-exposed cells and control cells using the following methods: compare_means *t*-test function from the ggpubr R package (Kassambara, 2020), weighted means permutation test and Kolmogorov-Smirnov Tests from the stats R package (R Core Team, 2021). FindMarkers from the Seurat R package was used to perform DE analysis between



groups. For DE between exposure groups and controls at each Day after filtering out genes encoding ribosomal proteins (Figures 5H, 6A), thresholds were set to the following: min. pct = 0.2, min. diff.pct = -Inf, logfc. threshold = 0.35. Genes with an adjusted p -value < 0.05 were considered significant. GO analysis was performed using the DEenrichRPlot function of the mixscape R package with the “GO_Biological_Process_2018” database with the following thresholds: logfc. threshold = 0.35, max genes = 500 (Supplementary Figures S5D–G).

2.10 Open-access web applications

Datasets can be browsed and visualized in open-access web applications at <https://neuroomicsexplorer.medisin.uio.no>.

Bulk RNA-seq and DNAm data: <https://neuroomicsexplorer.medisin.uio.no/bulkCitNeuronalDiff>. The bulkCitNeuronalDiff web application contains five tabs. “bulkCitNeuronalDiff app information” provides a short description of the methods used and a graphical abstract. “Explore GE results” allows the user to select a results file from the bulk differential gene expression analysis

to explore, either comparisons between days in control cells, citalopram dose-response (DR) or citalopram time-response (TR) analysis. The results are viewed in a searchable data table in addition to a statistics histogram and volcano plots with gene information at each point. The user can filter data on significance level, download plots as PDF files and tables as CSV files. “Explore DNAm results” has the same functionality as “Explore GE results”, applied to the bulk differential DNAm analysis results. Here, only data with $\text{FDR} < 0.05$ is shown to improve speed of the application. “GE boxplots” and “DNAm boxplots” provides functionality to plot time- and dose-response plots for gene expression and DNAm data equivalent to those in Figures 2–4. Here, the user can search for any gene or CpG, select linear or non-linear line type, subset data on group, day, (citalopram) concentration or treatment, and download plots as PDF files.

Single-cell data: <https://neuroomicsexplorer.medisin.uio.no/scRNACitNeuronalDiff>. The scRNACitNeuronalDiff web application contains seven tabs, which provides functionality to visualize the scRNA data in different ways. “CellInfo vs GeneExp” allows the user to plot two principal component (PC), t-distributed Stochastic Neighbor Embedding (tSNE), or Uniform Manifold

Approximation and Projection (UMAP) plots side-by-side, colored by various cell information metadata, such as original identity, day, cell cycle phase or different clustering parameters, as well as the gene expression of any selected gene. In the “CellInfo vs CellInfo” and “GeneExp vs GeneExp” tabs, the user can plot either two cell information plots or two gene expression plots side-by-side, respectively. In the “Gene coexpression” tab, co-expression of two selected genes can be plotted together in the same PCA, tSNE or UMAP. In the “Violinplot/Boxplot” tab, the user can plot cell information on the X-axis and cell information or gene expression of any selected gene on the Y-axis of a violin plot or boxplot. In the “Proportion plot” tab, the proportion or number of cells can be plotted for available cell information, and finally in the “Bubbleplot/Heatmap” tab gene expression in up to 50 genes can be plotted together in a bubbleplot or heatmap. In each tab, the user can subset data based on cell and all plots can be downloaded as PDF or PNG files.

2.11 Statistical analysis

Statistical analyses were performed in R version 4.2 (R Core Team, 2021) using edgeR (Robinson et al., 2010), Limma (Ritchie et al., 2015), Seurat (Stuart et al., 2019; Hao et al., 2024), ggpubr (Kassambara, 2020) and stats (R Core Team, 2021) packages. Details are described in the relevant methods above.

3 Results

3.1 Experimental set-up and validation of neuronal differentiation of hESCs

We hypothesized that early exposure to citalopram affects DNAm and regulation of the genes involved in neuronal differentiation. To comprehensively study the effect of citalopram on the epigenetic and transcriptional profiles in a model of early human neurodevelopment, we used a neuronal differentiation protocol optimized for neurotoxicology studies recently published by our group (Samara et al., 2022a; 2022b) (Figure 1A). The hESCs were exposed to physiological concentrations of citalopram (50, 100, 200 and 400 nM, reflecting human therapeutic doses (Hendrick et al., 2003; Rampono et al., 2009; Paulzen et al., 2017; Hiemke et al., 2018)) from Day 1 and throughout differentiation to Day 13 to model the effect of daily maternal intake of citalopram on neurodevelopment in the first trimester. The selected concentrations of citalopram did not affect hESC viability after 24 h of exposure (Figure 1B). There were no visually detectable morphologic differences between cells exposed to citalopram and unexposed control cells at any stage (Supplementary Figure S1). Flow cytometric analysis confirmed that the transcription factor OCT4, involved in establishment and maintenance of pluripotency, was present at Day 0 and absent at Day 13 in both unexposed control cells and cells exposed to 400 nM (Cit400) citalopram (Figure 1C). The levels of neural progenitor marker SOX1 increased at Day 13 compared to Day 0. Similarly, the levels of tubulin beta class III (TUBB3), a structural cytoskeletal protein involved in neurogenesis, and cell adhesion protein NCAM1, a regulator of neurogenesis,

neurite outgrowth and cell migration, increased at Day 13. Exposure to Cit400 did not affect the presence of these markers at Day 13.

To validate the neuronal differentiation process in the protocol, we performed differential gene expression and DNAm analyses in control samples between Day 0, Day 6, Day 10 and Day 13. These data have been made available in a web tool [bulkCitNeuronalDiff](#), enabling browsing and visualization of differential analysis, gene expression and DNAm levels. As expected, major changes in gene expression and DNAm occurred during neuronal differentiation of the control cells (Supplementary Figures S2, S3 and [bulkCitNeuronalDiff](#)), and samples clustered according to Day (Supplementary Figures S2A, B). To assess whether the differentiation was affected by the higher initial cell seeding and if differentiation corresponded with our group's recently published data (Samara et al., 2022b), we identified overlapping differentially expressed genes (DEGs) and differentially methylated CpGs (DMCs) between Day 0 and 13 (Supplementary Figures S2C, D). Of the DEGs and DMCs identified in the present study, 83% and 75% overlapped with Samara and Spildrejorde et al. (Samara et al., 2022b), respectively. There were also many unique DEGs and DMCs in the present study, which could indicate some batch effects, either during differentiation, and/or at later steps. Volcano plots for gene expression and DNAm are shown in Supplementary Figures S2E, F and top DEGs heatmaps between Days are shown in Supplementary Figure S2G.

Many of the top shared biological processes (BPs) for both gene expression changes (Supplementary Figure S3A) and DNAm changes (Supplementary Figure S3B) during differentiation included relevant terms for neuronal differentiation, such as *developmental induction*, *neuron differentiation* and *nervous system development*. The DEGs overlapped with differentially methylated genes (DMGs) at the different stages (Supplementary Figures S3C–E), thus showing good correspondence between datasets. The number of DEGs and DMCs overlapping between stages are shown in Supplementary Figures S3F, G. Expression of pluripotency marker genes such as *POU5F1*, *NANOG* and *LIN28A* decreased after Day 0, whereas neuronal differentiation marker genes such as *OTX2*, *MAP2*, *NEUROD1*, *STMN2*, *TUBB3* and *FOXG1* increased during differentiation (Supplementary Figure S2H).

3.2 Citalopram affects gene expression and DNAm levels over time during neuronal differentiation

Using bulk RNA-seq, we first examined the expression of serotonin receptors in both control and citalopram-exposed cells. Some of the genes encoding serotonin receptors were present at Day 0, albeit very lowly expressed throughout differentiation (*HRT1A*, *HRT1B*, *HRT1F*, *HRT3A* and *HRT7*; not shown). Expression of *HTR1D* and *HTR2A* peaked at Day 6 and decreased during differentiation, whereas expression of *HTR2C* increased during differentiation (Figure 2A), confirming the transcriptional presence of serotonin receptors.

To study whether exposure to citalopram caused gene expression or DNAm changes over time during neuronal

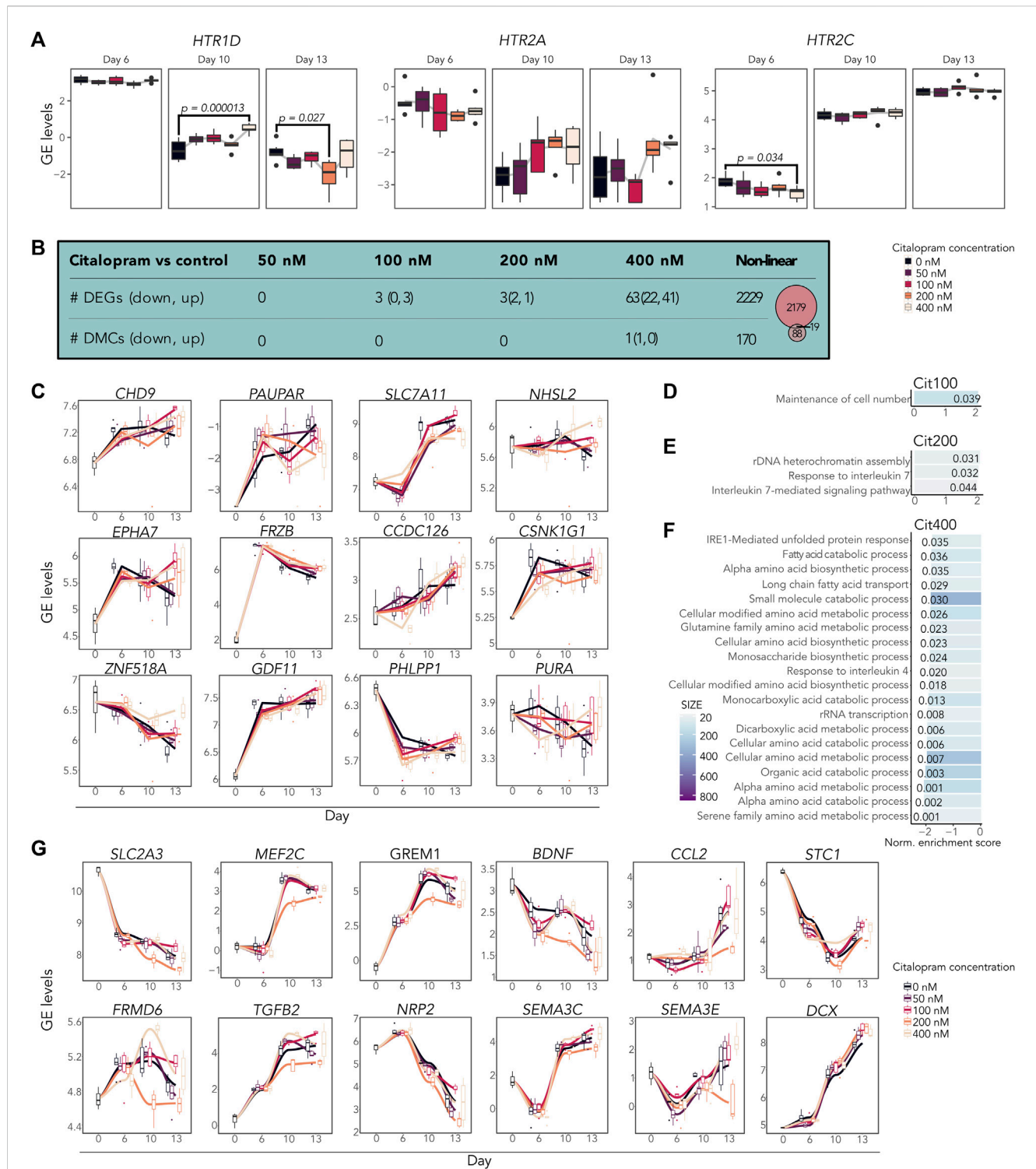
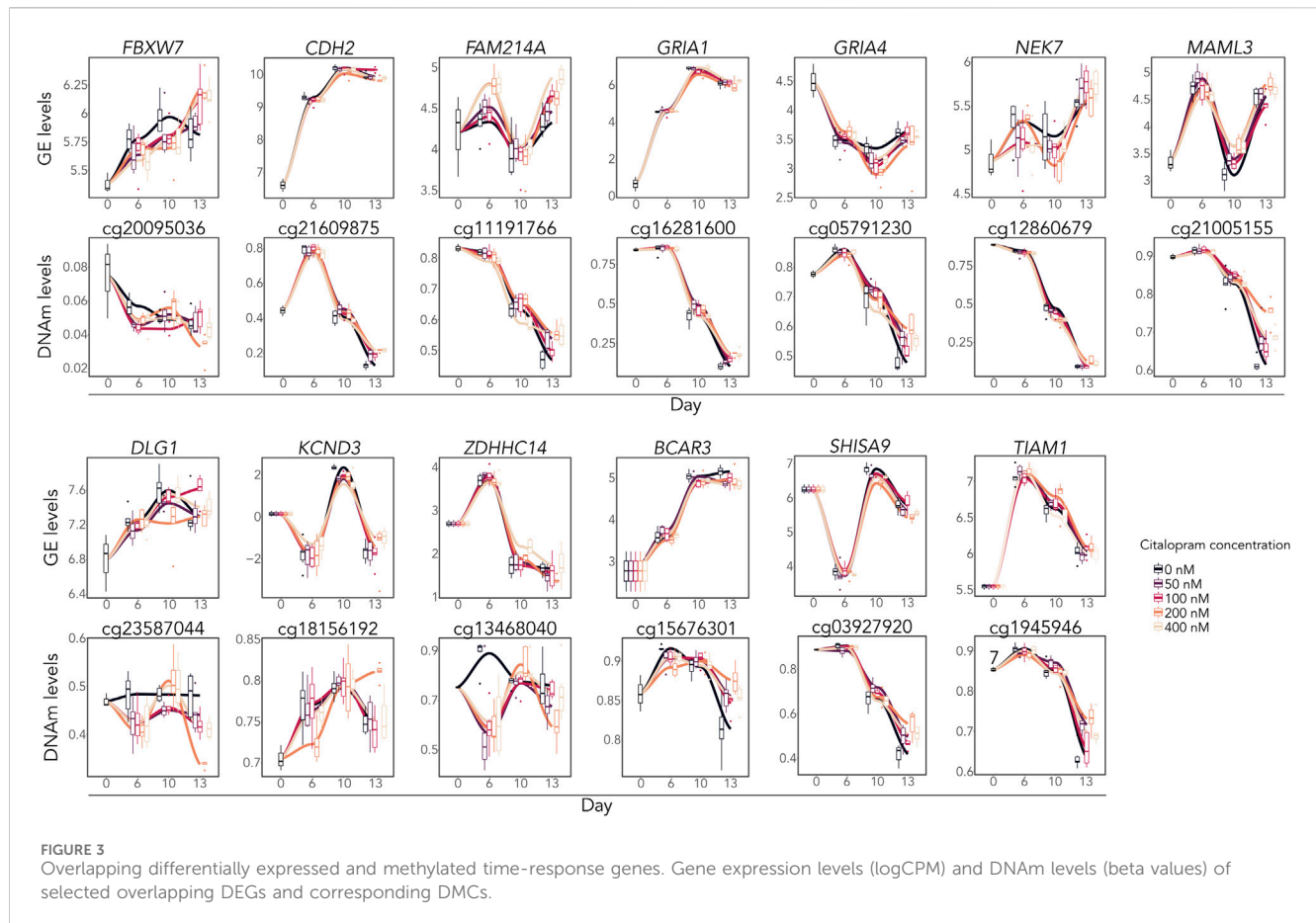


FIGURE 2 Time-response of citalopram-exposure during neuronal differentiation of hESCs. **(A)** Gene expression (GE) levels (log counts per million, logCPM) of selected serotonin receptor genes for Day 6 to Day 13. **(B)** Table showing the number of genes and CpGs that responded to the different concentrations of citalopram over time (Day 6 to Day 13). Venn diagram showing overlapping DEGs and DMCs. **(C)** GE levels (logCPM) of selected linear time-response DEGs. **(D–F)** Shared biological processes (BPs) among genes that were differentially expressed in cells exposed to **(D)** 100 nM, **(E)** 200 nM or **(F)** 400 nM citalopram over time. **(G)** GE levels (logCPM) of selected non-linear time-response DEGs. Genes with adjusted p -value < 0.05 were considered significant.

differentiation of hESCs, we performed a linear time-response analysis and compared each concentration of citalopram from Day 6 to Day 13 to unexposed control cells using bulk omics

data (Figure 2 and bulkCitNeuronalDiff). Only one position annotated to *RABEP2* was differentially methylated between 400 nM citalopram and control over time (Figure 2B and

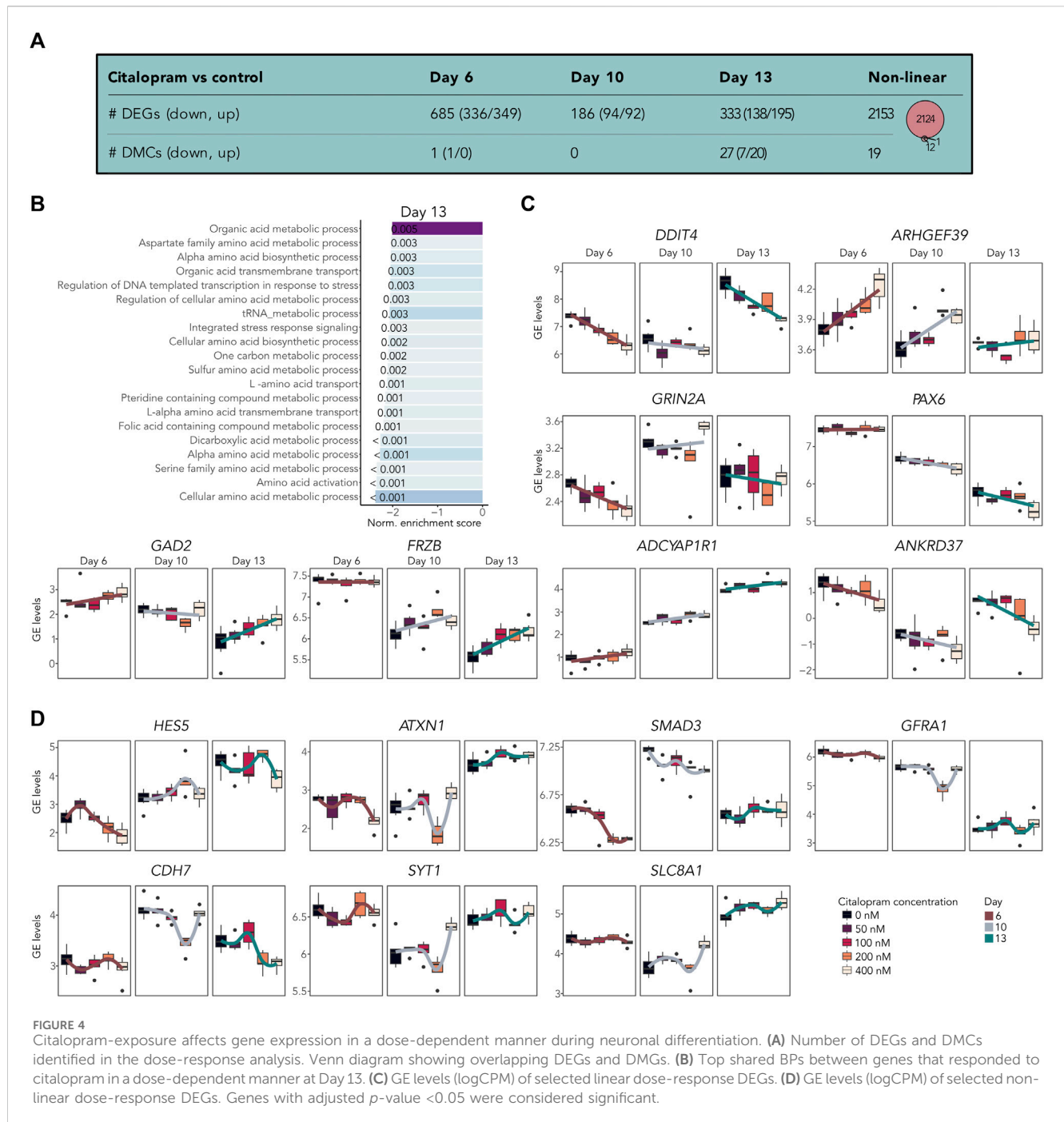


bulkCitNeuronaldiff). In contrast, we observed a dose-dependent linear effect of citalopram exposure on the number of DEGs (Figure 2B and **bulkCitNeuronaldiff**). Differentiating cells exposed to 50 nM citalopram (Cit50) did not show any differential expression compared to control over time (Figure 2B). However, exposure to 100 (Cit100) and 200 nM citalopram (Cit200) resulted in three DEGs, whereas Cit400 resulted in 63 DEGs.

Among the DEGs identified was the chromatin remodeler *CHD9*, which was upregulated in Cit100 cells compared to controls. *PAUPAR*, a gene encoding a long non-coding RNA that regulates *PAX6* (Vance et al., 2014), and *SLC7A11*, associated with ASD (Rojas-Charry et al., 2021), was significantly downregulated in Cit400 cells over time (Figure 2C). In contrast, *NHSL2* (associated with ASD (Gerges et al., 2022)), *EPHA7* (important for neuronal maturation and synaptic function (Clifford et al., 2014)), WNT antagonist *FRZB*, *CCDC126* (associated with depression (Gui et al., 2018)), *CSNK1G1* (involved in glutamergic neurotransmission (Chergui et al., 2005)), transcriptional regulator *ZNF518A*, *GDF11* (a growth factor involved in neurogenesis and differentiation of neuronal subtypes (Shi and Liu, 2011)) and *PURA* (essential to neurodevelopment and linked to neuroprotection (Daniel and Johnson, 2018; Molitor et al., 2021)) were upregulated in Cit400 cells over time (Figure 2C). *PHLPP1* was differentially expressed over time in both Cit100, Cit200 and Cit400 compared to controls.

Interestingly, *PHLPP1* is involved in many important functions in the nervous system, including memory formation, cellular survival and proliferation (Mallick et al., 2022). Further, we performed GSEA analysis to elucidate if the DEGs identified between citalopram-exposed and unexposed control cells shared any biological functions (Figures 2D–F). Results from this analysis revealed enrichment of different metabolic and catabolic processes, including fatty acid and amino acid biosynthetic processes among the DEGs.

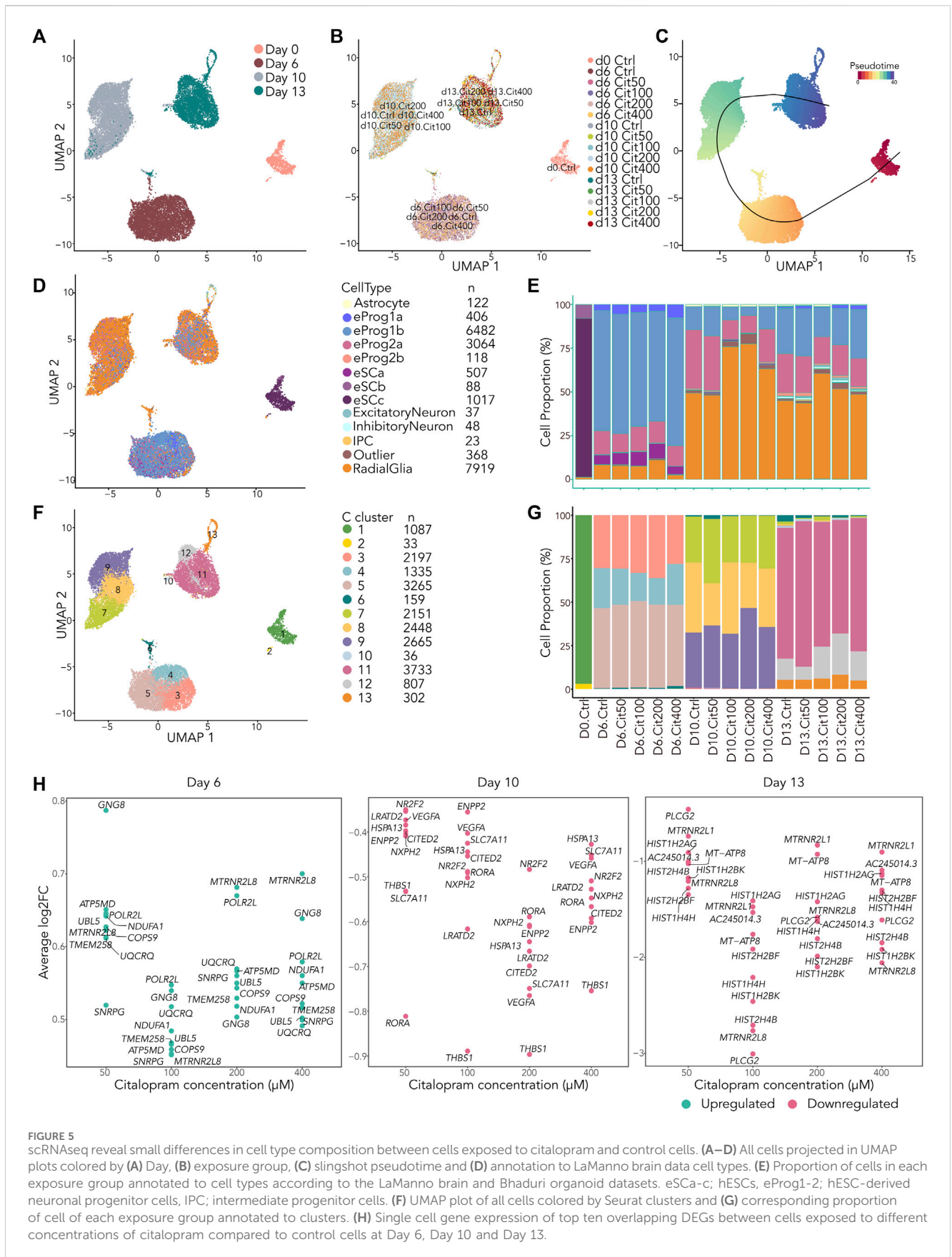
Citalopram may also induce non-monotonic responses due to complex pharmacodynamic processes (Ludden, 1991). Using a non-linear regression model to identify time-dependent effects of citalopram, 2,229 genes were differentially expressed in citalopram-exposed cells at all concentrations compared to controls (Figure 2B). The DEGs included genes involved in neuronal development and brain function, such as *FRMD6* (involved in neuronal differentiation (Chen et al., 2021)), *SLC2A3* (a neural glucose transporter (Ziegler et al., 2020)), *GREM1* (antagonist of bone morphogenic protein (Ichinose et al., 2021)), *MEF2C* (important for neuronal differentiation and axogenesis (Zhang and Zhao, 2022)), *TGFB2* (essential for neurodevelopment (Meyers and Kessler, 2017)) and *DCX* (involved in neuronal migration (Ayanlaja et al., 2017)) (Figure 2G). Further, *NRP2*, *SEMA3C* and *SEMA3E*, involved in axon guidance during neurodevelopment (Oh and Gu, 2013), were downregulated in Cit200. Some DEGs linked to depression and neuroinflammation (*BDNF* (Porter and O'Connor, 2022),



CCL2 (Curzytek and Leśkiewicz, 2021), *STC1* (Chao et al., 2021), *MEF2C* (Hyde et al., 2016)) were also downregulated in Cit200 over time (Figure 2G). The levels of the non-linear DEGs fluctuate with day and concentration, thus the biological interpretation is difficult. However, many of the DEGs are dysregulated in Cit200 compared to controls, suggesting that this concentration has a substantial effect on cells undergoing neuronal differentiation.

DNAm analysis showed that citalopram induced non-linear time-dependent changes at 170 CpGs, annotated to 107 genes. No significant gene ontology terms were identified. Of the 107 DMGs,

19 overlapped with DEGs (Figures 2B, 3). Some of the overlapping genes are involved in processes crucial for neurodevelopment (*FBXW7* (Yang et al., 2021), *CDH2* (László and Lele, 2022)), neuroinflammation (*NEK7* (Chen et al., 2019)), neuronal excitability (*ZDHHC14* (Sanders et al., 2020)), synaptic plasticity (*SHISA9* (Kunde et al., 2017)), neurite outgrowth (*TIAM1* (Ehler and Salinas, 1997)) and neurotransmission (*DLG1* (Marziali et al., 2019), voltage-gated potassium channel *KCND3*, glutamate receptors *GRIA1* and *GRIA4*) (Figure 3). Further, genes linked to mood disorders and stress response were identified (*BCAR3* (Han et al., 2020), *FAM214A* (Witte et al., 2022), *MAML3* (Kuehner et al., 2023)).



3.3 Citalopram exposure induces dose-dependent changes in gene expression during neuronal differentiation

To assess the dosage-effect of citalopram, we performed a bulk RNA-seq dose-response analysis. To identify both potential monotonic and non-monotonic responses, we tested both the linear and non-linear effect of increasing citalopram concentrations compared to control cells (Figure 4 and [bulkCitNeuronalDiff](#)). Employing the linear regression model for each differentiation day we identified 685 DEGs associated with citalopram exposure in a dose-dependent manner compared to control cells at Day 6. At Day 10 and 13, we identified 186 and 333 DEGs, respectively compared to Day 6, which was baseline in this comparison (Figure 4A). GSEA did not identify any significant shared BPs for dose-response genes at Day 6 or Day 10. At Day 13, however, BPs related to metabolic and catabolic processes were enriched (Figure 4B). Interestingly, some of the linear dose-response DEGs have been implicated in transmission and plasticity (*GRIN2A* (Paoletti et al., 2013), *GAD2* (Pan, 2012)), depression and antidepressant effect (*DDIT4* (Wang et al., 2018), *GAD2* (Unschuld et al., 2009)) anxiety and stress responses (*ADCYAP1R1* (Oyola and Handa, 2017; Wang et al., 2021)), WNT signalling (*FRZB* (Mitsiadis et al., 2017)), neurogenesis (*ARHGEF39* (Anijs et al., 2022)) and hippocampal volume (*ANKRD37* (Xu et al., 2022)) (Figure 4C). Further, linear differential DNAm analysis identified one DMC at Day 6 (*RABEP2*), none at Day 10 and 27 at Day 13 (annotated to, e.g., *MECOM*, *GRIN1*, *SORCS2*; Figure 4A and [bulkCitNeuronalDiff](#)).

The non-linear dose-response analysis identified 2,153 DEGs (Figures 4A,D and [bulkCitNeuronalDiff](#)). Most of these were also identified in the non-linear time-response analysis (n = 1703). We identified DEGs implicated in cell state transitioning in neural progenitor (*HES5* (Manning et al., 2019)), neuronal differentiation (*CDH7* (Feng et al., 2017)), neurogenesis (*SMAD3* (Hiew et al., 2021)), synaptic plasticity (*GFRA1* (Bonafina et al., 2019)), synaptic transmission (*SYT1* (Riggs et al., 2022)), neuronal ion homeostasis (*SLC8A1* (Blaustein and Lederer, 1999)) and memory and learning (*ATX1* (Lu et al., 2017)). Further, citalopram induced non-linear time-dependent changes at 19 DMCs, annotated to 13 genes (Figure 4A and [bulkCitNeuronalDiff](#)). Of the DMGs, one overlapped with DEGs (*GRIA1*, Figure 3). Overall, genes involved in brain function were dose-dependently dysregulated in cells exposed to citalopram.

3.4 Effect of citalopram exposure at different stages during neuronal differentiation

In addition to the longitudinal and dose effects of citalopram exposure on gene expression and DNAm changes during differentiation, citalopram might exert more specific effects at different stages and within distinct cell-types. To identify dose-dependent cell-type specific gene expression signatures and potential alterations in cell type composition during differentiation, we also performed single-cell RNA sequencing

(scRNAseq) at the four different timepoints (Day 0, 6, 10 and 13) (Figure 5 and [Supplementary Figure S4](#)). These data have been made available for browsing and visualization in a web tool “scRNA citalopram-exposure during neuronal differentiation of hESCs” ([scRNACitNeuronalDiff](#)).

After filtering of the data, a total of 20,217 cells were included in downstream analysis ([Supplementary Figure S4A](#)). As expected, cells clustered according to differentiation day (Figures 5A and [Supplementary Figure S4C](#)), whereas exposed and unexposed cells clustered together at each day (Figure 5B). The cells were ordered according to their pseudotime development using Slingshot (Street et al., 2018), confirming that pseudotime differentiation values increased from Day 0 to Day 13 (Figures 5C and [Supplementary Figure S4D](#)) reflecting progression through the differentiation process.

We used SingleR (Aran et al., 2019) and compared the cells to the scRNA La Manno brain dataset (LaManno et al., 2016) and the Bhaduri forebrain organoid dataset (Bhaduri et al., 2020). This revealed that most cells at Day 6 were classified as neuronal progenitors (LaManno et al., 2016), with some variation in the progenitor subtype depending on citalopram concentration (Figures 5D, E). At Day 10 and 13, most cells were classified as radial glia cells (Bhaduri et al., 2020), whereas a smaller proportion were classified as neuronal progenitors. In addition, at Day 13, a small proportion of cells were more differentiated, classified as intermediate progenitor cells, excitatory neurons and inhibitory neurons (Bhaduri et al., 2020). In control cells, expression of selected marker genes involved in neurodifferentiation at Day 13 were comparable with Day 13 in the Samara and Spildrejorde et al. study ([Supplementary Figure S4E](#)) (Samara et al., 2022b).

The cells resolved into 13 Seurat clusters at resolution 0.55 (Figures 5F, G and [Supplementary Figures S4F–G](#)), where pseudotime differentiation progressed from C1 to C11-13 ([Supplementary Figure S4H](#)). The top five DEGs for each cluster are visualized in [Supplementary Figure S4I](#). Overall, these clusters and expression of genes confirm neuronal differentiation of the citalopram-exposed cells and control cells. There was some variation in cell proportions within the different clusters depending on exposure to citalopram or not. However, no specific dose- or time-dependent trend was found (Figure 5G).

Next, we investigated whether the scRNA dataset revealed any dose-dependent DEGs. These analyses identified overlapping DEGs between citalopram and control cells at all citalopram concentrations (Figure 5H). At Day 6, the top ten overlapping DEGs were upregulated in citalopram-exposed cells. Of these, genes involved in neuroinflammation (*COPS9* (Tian et al., 2023)), neuroprotection (*MTRNR2L8* (Karachaliou and Livanou, 2023)) and mitochondrial function (*ATP5MD*, *NDUFA1*, *UQCRCQ*) were identified. Interestingly, mitochondrial function is important for neurodevelopment, and dysfunction is known to play a crucial role in the pathogenesis of depression (Song et al., 2023). In contrast, at Day 10 and Day 13, the top ten overlapping DEGs were downregulated in citalopram-exposed cells. At Day 10, genes involved in neurodevelopment (*CITED2* (Wagner and MacDonald, 2021), *RORA* (Ribeiro and Sherrard, 2023), *NR2F2* (Tocco et al., 2021)), neuronal migration (*THBS1* (Blake et al., 2008)) and synaptic function (*VEGFA* (Licht et al., 2009)) were identified. Further, the glutamate transporter *SLC7A11* that was also

A

Day	Citalopram vs control	50 nM	100 nM	200 nM	400 nM
6	# DEGs (down, up)	60 (45/15)	9 (7/2)	116 (59/57)	831 (512/319)
	# scDEGs (down, up)	229 (106/123)	65 (11/54)	193 (128/65)	140 (4/136)
	# DMCs (down, up)	0	0	0	0
10	# DEGs (down, up)	27 (16/11)	0	1072 (663/409)	529 (221/308)
	# scDEGs (down, up)	30 (19/11)	814 (813/1)	831 (823/8)	357 (330/27)
	# DMCs (down, up)	0	0	0	0
13	# DEGs (down, up)	18 (15/3)	4241 (2748/1493)	488 (258/230)	1704 (935/769)
	# scDEGs (down, up)	179 (134/45)	401 (321/80)	91 (35/56)	151 (78/73)
	# DMCs (down, up)	0	0	2(0/2)	2(1/1)

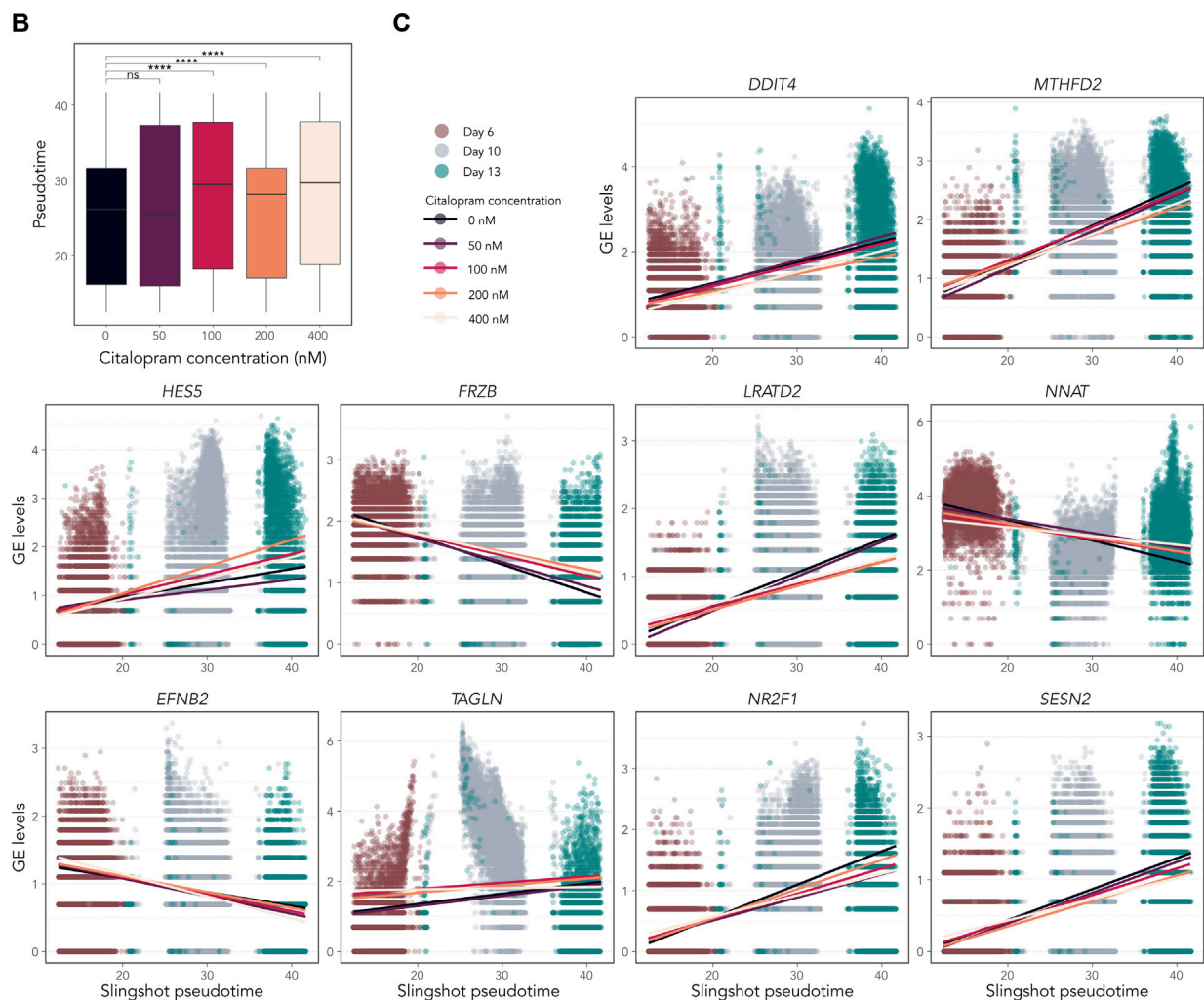


FIGURE 6 Temporally expressed genes respond differently in citalopram-exposed cells compared to control cells during differentiation. **(A)** Pairwise comparisons between citalopram and control for RNA-seq (DEGs), scRNAseq (scDEGs) and DNAm (DMCs) at Day 6–13. **(B)** Boxplot of Slingshot pseudotime values per exposure group for Day 6–13. Significant comparisons are marked with asterisks (Student’s t-test, ****: $p \leq 0.0001$). **(C)** GE levels (logcounts) of *DDIT4*, *MTHFD2*, *HES5*, *FRZB*, *LRATD2*, *NNAT*, *EFNB2*, *TAGLN*, *NR2F1* and *SESN2* selected from the top 100 temporally expressed genes, which responded differently in citalopram-exposed and control cells across Slingshot pseudotime at Day 6–13. Each dot represents one cell, and the lines represent the average GE for each citalopram concentration across pseudotime.

identified in the bulk time-response analysis (Figure 2C), was downregulated at Day 10. At Day 13, genes involved in mitochondrial function (*MT-ATP8*), genes associated with neuroprotection (*MTRNR2L8*, *MTRNR2L1* (Karachaliou and Livaniou, 2023)), and genes encoding histone variants (*HIST2H2BF*, *HIST1H4H*, *HIST1H2BK*, *HIST1H2AG*) were identified. Of note, *HIST1H2AG*, has previously been associated with depression (Tirozzi et al., 2023).

We also performed pairwise differential analyses of bulk RNA-seq, scRNAseq and DNAm datasets to identify gene expression and DNAm differences between each concentration of citalopram compared to control at Day 6, 10 and 13 (Figure 6A and bulkCitNeuronalDiff). Four DMCs were identified in the DNAm analysis, suggesting that each dose of citalopram appears to have minor effect on DNAm at each neuronal differentiation stage (bulkCitNeuronalDiff). Cit200 had increased DNAm at CpGs annotated to *EYS* and *LAT* compared to control. Cit400 had decreased and increased DNAm at CpGs annotated to *DGKA* and *SLC30A8* compared to control, respectively. However, the expression of these genes was not changed at Day 13.

We identified varying numbers of DEGs at each Day between control and citalopram in both bulk and scRNAseq data (Figure 6A and bulkCitNeuronalDiff), some of which were specific for citalopram and controls, whereas others overlap between several citalopram concentrations (Supplementary Figures S5A–C). Furthermore, similar GO terms related to mitochondrial function, and different metabolic and catabolic processes (Supplementary Figure S5D) were common among the top enriched BPs between different comparisons, in the scRNA analyses. At Day 10, downregulated terms involved in regulation of transcription and stress response were identified (Supplementary Figure S5D). At Day 13, more BPs involved in chromatin organization, catabolic and metabolic processes were enriched, in addition to upregulation of *central nervous system development*, *axon development* and *generation of neurons* in Cit200 cells compared to controls.

3.5 Citalopram enhances differentiation

To investigate if citalopram induced changes in the pseudotemporal ordering of the cells, differential topology analysis of the slingshot trajectory was performed. After removing Day 0 from the dataset, a subtle but significant difference in pseudotime differentiation was observed between citalopram-exposed cells and control cells (Figure 6B). Specifically, citalopram-exposed cells had higher mean pseudotime levels compared to control cells, irrespective of differentiation day. This result was confirmed using a more robust permutation test (Supplementary Figure S6A) and Kolmogorov-Smirnov test (p -values 5.5×10^{-4} , $<2.2 \times 10^{-16}$, 2.2×10^{-16} , $<2.2 \times 10^{-16}$, for 50, 100, 200 and 400 nM citalopram compared to control cells, respectively). These results suggest that citalopram exposure subtly enhances neuronal differentiation of hESCs.

Some temporally expressed genes (Supplementary Figure S6B) responded differently to citalopram exposure compared to control cells (Figure 6C and Supplementary Figure S6C). For *CHAC1*, *LRATD2*, *ENFB2*, *TAGLN*, *NE2F1*, *SESN2*, *TPM1*, *CARS*, *VEGFA*, *XBPI*, *DDIT4* and *HCRT* expression was decreased in citalopram-

exposed cells compared to control cells in more differentiated cells. In contrast, *HES5*, *FRZB* and *NKX2-1* expression was increased in citalopram-exposed cells compared to more differentiated control cells. Further, *NNAT*, which is involved in intracellular signalling critical for differentiation, synaptogenesis and plasticity (Lin et al., 2010; Oyang et al., 2011) was upregulated in citalopram-exposed cells. Interestingly, *LRATD2* and *NNAT* have previously been linked to electroconvulsive therapy response in depressed patients (Sirignano et al., 2021). The scRNA pseudotime analysis identified genes also found in the bulk RNA-seq dose-response analysis (Figures 4C, D), such as *DDIT4*, *HES5* and *FRZB* (Figure 6C).

4 Discussion

We aimed to investigate the impact of maternal citalopram use in early embryonic neurodevelopment using a neuronal differentiation model, which has been optimized for neuropharmacology studies (Samara et al., 2022a; 2022b). The hESCs were exposed to therapeutic concentrations of citalopram from differentiation Day 1–13. The results presented in this study provide valuable insights into the effects of citalopram exposure on gene expression and DNAm during the initial stages of neuronal differentiation. To our knowledge, this is the first multi-omics analysis of citalopram-exposed differentiating hESCs.

The analyses of gene expression and DNAm changes during neuronal differentiation revealed significant changes in the unexposed control cells, consistent with the expected patterns of neuronal differentiation. Many DEGs and DMCs were associated with BPs related to neuronal differentiation and nervous system development and overlapped with the study by Samara and Spildrejorde et al. (Samara et al., 2022b). However, there were also unique DEGs and DMCs to this study, highlighting the importance of using internal controls for each neurotoxicology experiment. Taken together, these results confirmed neuronal differentiation, and the Day 6 and Day 10 cells adds to the knowledge of temporally waves of gene expression during the neural rosette stage and self-patterning phase of neuronal differentiation (Samara et al., 2022b). Further, serotonin receptors, implicated in depression aetiology and SSRI response (Nautiyal and Hen, 2017), were expressed in both controls and citalopram-exposed cells, suggesting that the cells in the neuronal differentiation model have potential to respond to serotonin signalling. However, serotonin levels were not measured, and cells did not express the serotonin transporter *SLC6A4*. Thus, studying citalopram exposure in this model may reflect indirect effects.

We identified citalopram-induced time- and dose-response effects on the expression of specific genes involved in neurodevelopment, neuronal migration, axon guidance, neuronal maturation, synaptic transmission, cell state transitioning and stress-response, which provides important insights into the molecular mechanisms underlying the potential effects of citalopram exposure on early brain development. Dysregulation of such crucial genes may potentially have an impact on cognitive and behavioural processes.

Interestingly, we also identified citalopram-induced time- and dose-response effects on the expression of genes

associated with depression aetiology and potential therapeutic mechanisms. For example, *CCL2* (*MCP-1*), a chemokine involved in a range of neurobiological processes, has been associated with depression brain-immune system communication and suggested as a potential antidepressant target (Curzytek and Leśkiewicz, 2021). Similarly, *BDNF*, a growth factor involved in neuroinflammation, has been indicated in depression pathogenesis and antidepressant efficacy (Porter and O'Connor, 2022). Also, *STC1* has been shown to decrease neuroinflammation and attenuate depression-like symptoms in rats (Chao et al., 2021). These findings suggest that citalopram may influence key pathways and processes implicated in depression, such as neuroplasticity, neuroinflammation, cellular stress response and neurotransmitter regulation (Saveanu and Nemeroff, 2012).

The time- and dose-response analysis of bulk RNA revealed differentially expressed genes in citalopram-exposed cells compared to control cells, sharing BPs involved in amino acid metabolic and catabolic processes. This result is in line with previous studies where changes in plasma amino acids have been identified as response to SSRI treatment (Kaddurah-Daouk et al., 2013; Woo et al., 2015), also evident for (es)citalopram (MahmoudianDehkordi et al., 2021). In addition to being building blocks in biosynthetic and metabolic processes, amino acids are also involved with synaptic neurotransmission. Understanding how antidepressants affect these may aid the understanding of depression aetiology and treatment response.

Hippocampal impairment has been associated with major depression disorder (MacQueen and Frodl, 2010). Citalopram exposure induced changes in *ANKRD37* and *GDF11*, important for hippocampal volume (Xu et al., 2022; Moigneu et al., 2023). Interestingly, in mice, infusion of *GDF11* enhanced hippocampal neurogenesis and attenuated depression-like symptoms (Moigneu et al., 2023). Further, a causal negative correlation between *ANKRD37* expression and hippocampal volume has been previously identified (Xu et al., 2022). The present study identified increased expression of *GDF11* and decreased expression of *ANKRD37*, suggesting that citalopram may potentially mediate its therapeutic action through hippocampal recovery. This result is consistent with several previous studies, where antidepressants have been reported to enhance hippocampal neurogenesis (Malberg et al., 2000; Anacker et al., 2011; Perera et al., 2011; Mateus-Pinheiro et al., 2013).

We also identified genes associated with NDDs such as ASD (e.g., *SLC7A11*, *NHSL2*, *PAX6*, *CDH2*, *ATX1*) and ADHD (e.g., *CDH2*), suggesting a potential link between citalopram exposure and the molecular pathways involved in the pathogenesis of NDDs. For example, altered expression of *SLC7A11* may disrupt amino acid transport and redox balance, which have been implicated in ASD pathogenesis (Rojas-Charry et al., 2021). Further, dysregulation of *CDH2* may disrupt synaptic function, indicated in ASD (László and Lele, 2022). Overall, the time- and dose-response results indicate that citalopram affects molecular mechanisms important during fetal neurodevelopment. In contrast, the corresponding DNAm analysis identified relatively few significant changes. We identified 19 genes with changes in both gene expression and DNAm, indicating that the citalopram-induced gene expression changes were modulated by other mechanisms other than DNAm, by

CpGs not covered by the EPIC array, or by CpGs which we did not have enough power to detect.

To gain a more detailed understanding of the effects of citalopram exposure at different stages of neuronal differentiation and within specific cell-types, scRNA-seq was performed. The analysis identified distinct cell clusters corresponding to the different stages of differentiation. The scRNA-seq analysis revealed dose-dependent cell-type specific gene expression signatures. For example, citalopram exposure increased expression of *FRZB*, involved in WNT signalling (Mitsiadis et al., 2017). The citalopram-induced increase in *FRZB* expression was identified in both bulk RNA-seq time- and dose-response analysis and in scRNA-seq pseudotime analysis. Interestingly, *FRZB*, was downregulated in paracetamol-exposed cells using the same neuronal differentiation model, albeit at different time points (Spildrejorde et al., 2023), indicating that the WNT-pathway respond differently to citalopram compared to paracetamol. Another gene that was differentially expressed in both paracetamol-exposed cells and citalopram-exposed cells was neuronal transcription factor *PAX6*. In paracetamol-exposed cells *PAX6* was upregulated, indicating a delay in neuronal differentiation (Spildrejorde et al., 2023). In contrast, *PAX6* expression was downregulated in citalopram-exposed cells in a dose-dependent manner, suggesting that citalopram may enhance neuronal differentiation. This is also in line with the pseudotemporal analysis, showing that citalopram-exposed cells were more differentiated compared to control cells. Interestingly, the SSRI sertraline has also shown to increase *DCX* expression indicating enhanced neuronal differentiation (Anacker et al., 2011), consistent with the citalopram-induced increase in *DCX* at Day 10 and 13.

There are several limiting factors to this study. The complexity of neurodevelopment in the human brain cannot fully be recapitulated using a simplified *in vitro* hESC neuronal differentiation model. We could not account for fetal-fetal or maternal-fetal signalling interactions. Additionally, the study only examined the effects of citalopram during a narrow time window of neuronal differentiation and at selected concentrations. Using one hESC line and no phenotype model, exploring genetic susceptibility related to disease risk was beyond the scope of this study. Furthermore, the model may not be suitable to investigate citalopram therapeutic mechanism of action, thus the interpretation in that direction remain speculative. Further research is needed to delineate the effects of citalopram exposure at different stages of neurodevelopment and to investigate potential long-term consequences.

To comply with the Findability, Accessibility, Interoperability and Reusability (FAIR) principles, we share both bulk RNA-seq and DNAm (bulkCitNeuronalDiff) and scRNAseq data (scRNACitNeuronalDiff) in open-access user-friendly web applications. These provide interactive functionality for browsing results, visualising genes and CpGs, and downloading figures and tables, allowing the reader to explore the data easily, fostering transparency, reproducibility, and collaboration in scientific research.

There are several translational aspects of the results obtained from this protocol and findings in, for example, cord blood from children prenatally exposed to maternal citalopram use. First, it can provide mechanistic insights into how citalopram exposure may influence DNAm and gene expression patterns during neuronal development, helping researchers understand the potential molecular pathways

involved. Second, it can generate hypotheses for further investigation in cord blood studies, suggesting specific genes that may be altered in infants exposed to maternal citalopram use. Third, comparative analysis with findings in cord blood can identify overlapping genes and support a potential link between citalopram exposure, omics modifications and neurodevelopmental outcomes. Such findings could strengthen causal inference and clinical translation of findings in cord blood on early brain development. Last, it can serve as a potential basis for validating and replicating cord blood findings.

In conclusion, this study provides important insights into the effects of early citalopram exposure on gene expression and DNAm during neuronal differentiation. The findings highlight the time- and dose-dependent alterations in gene expression associated with neurodevelopment, axon guidance, neuronal maturation, synaptic transmission and depression. The study's multi-omics approach offers valuable mechanistic insights and potential translational implications. Overall, this study contributes to our understanding of citalopram's impact on early brain development and provides a basis for future investigations.

Data availability statement

The data presented in the study are deposited in the NCBI's GEO repository, accession number GSE260892 (Subseries RNA-seq: GSE260888, DNAm: GSE260890, scRNA-seq: GSE260889).

Ethics statement

Ethical approval was not required for the studies on humans in accordance with the local legislation and institutional requirements because only commercially available established cell lines were used.

Author contributions

MS: Conceptualization, Formal Analysis, Investigation, Methodology, Visualization, Writing–original draft, Writing–review and editing. ML: Conceptualization, Methodology, Writing–review and editing, Investigation. AS: Conceptualization, Methodology, Supervision, Writing–review and editing. HA: Methodology, Writing–review and editing, Data curation, Investigation. AS: Methodology, Writing–review and editing. GA: Resources, Writing–review and editing. HN: Project administration, Supervision, Writing–review and editing. KG: Conceptualization, Funding acquisition, Methodology, Project administration, Resources, Supervision, Writing–original draft, Writing–review and editing. RL: Conceptualization, Funding acquisition, Methodology, Project administration, Resources, Supervision, Writing–review and editing.

References

Anacker, C., Zunsain, P. A., Cattaneo, A., Carvalho, L. A., Garabedian, M. J., Thuret, S., et al. (2011). Antidepressants increase human hippocampal neurogenesis by activating the glucocorticoid receptor. *Mol. Psychiatry* 16, 738–750. doi:10.1038/mp.2011.26

Funding

The author(s) declare that financial support was received for the research, authorship, and/or publication of this article. We acknowledge funding from Research Council of Norway, grant 241117 (RL).

Acknowledgments

The sequencing service was provided by the Norwegian Sequencing Centre (<http://www.sequencing.uio.no/>), a national technology platform hosted by Oslo University Hospital and the University of Oslo and supported by the “Infrastructure” programs of the Research Council of Norway and the Southeastern Regional Health Authorities. PharmaTox Strategic Research Initiative was supported by Faculty of Mathematics and Natural Sciences, University of Oslo. We thank Manuela Zucknick at Oslo Centre for Biostatistics and Epidemiology, University of Oslo and Oslo University Hospital, for statistical advising regarding the time- and dose-response analysis. We thank the IT Department at UiO (USIT) for setting up and managing the web applications at neuroomicsexplorer.medisin.uio.no. We thank the Norwegian Centre for Stem Cell Research for discussions at the initiation of this project. We thank Oslo University Hospital for open access publication support. The funders played no role in study design, data collection, data analyses, interpretation, or writing of the article.

Conflict of interest

The authors declare that the research was conducted in the absence of any commercial or financial relationships that could be construed as a potential conflict of interest.

Publisher's note

All claims expressed in this article are solely those of the authors and do not necessarily represent those of their affiliated organizations, or those of the publisher, the editors and the reviewers. Any product that may be evaluated in this article, or claim that may be made by its manufacturer, is not guaranteed or endorsed by the publisher.

Supplementary material

The Supplementary Material for this article can be found online at: <https://www.frontiersin.org/articles/10.3389/fcell.2024.1428538/full#supplementary-material>

Andalib, S., Emamhadi, M. R., Yousefzadeh-Chabok, S., Shakouri, S. K., Høiland-Carlsen, P. F., Vafae, M. S., et al. (2017). Maternal SSRI exposure increases the risk of autistic offspring: a meta-analysis and systematic review. *Eur. Psychiatry* 45, 161–166. doi:10.1016/j.eurpsy.2017.06.001

- Anijs, M., Devanna, P., and Vernes, S. C. (2022). ARHGEF39, a gene implicated in developmental language disorder, activates RHOA and is involved in cell de-adhesion and neural progenitor cell proliferation. *Front. Mol. Neurosci.* 15, 39. doi:10.3389/fnmol.2022.941494
- Aran, D., Looney, A. P., Liu, L., Wu, E., Fong, V., Hsu, A., et al. (2019). Reference-based analysis of lung single-cell sequencing reveals a transitional profibrotic macrophage. *Nat. Immunol.* 20(2), 163–172. doi:10.1038/s41590-018-0276-y
- Aryee, M. J., Jaffe, A. E., Corrada-Bravo, H., Ladd-Acosta, C., Feinberg, A. P., Hansen, K. D., et al. (2014). Minfi: a flexible and comprehensive Bioconductor package for the analysis of Infinium DNA methylation microarrays. *Bioinformatics* 30, 1363–1369. doi:10.1093/bioinformatics/btu049
- Ayanlaja, A. A., Xiong, Y., Gao, Y., Ji, G., Tang, C., Abdullah, Z., et al. (2017). Distinct features of doublecortin as a marker of neuronal migration and its implications in cancer cell mobility. *Front. Mol. Neurosci.* 10, 199. doi:10.3389/fnmol.2017.00199
- Bhaduri, A., Andrews, M. G., Leon, W. M., Jung, D., Shin, D., Allen, D., et al. (2020). Cell stress in cortical organoids impairs molecular subtype specification. *Nature* 578, 142–148. doi:10.1038/s41586-020-1962-0
- Blake, S. M., Strasser, V., Andrade, N., Duit, S., Hofbauer, R., Schneider, W. J., et al. (2008). Thrombospondin-1 binds to ApoER2 and VLDL receptor and functions in postnatal neuronal migration. *EMBO J.* 27, 3069–3080. doi:10.1038/emboj.2008.223
- Blaustein, M. P., and Lederer, W. J. (1999). Sodium/calcium exchange: its physiological implications. *Physiol. Rev.* 79, 763–854. doi:10.1152/physrev.1999.79.3.763
- Bonafina, A., Trincherio, M. F., Rios, A. S., Bekinschtein, P., Schinder, A. F., Paratcha, G., et al. (2019). GDNF and GFRα1 are required for proper integration of adult-born hippocampal neurons. *Cell Rep.* 29, 4308–4319. doi:10.1016/j.celrep.2019.11.100
- Brummelte, S., Glanaghy, E. M., Bonnin, A., and Oberlander, T. F. (2017). Developmental changes in serotonin signaling: implications for early brain function, behavior and adaptation. *Neuroscience* 342, 212–231. doi:10.1016/j.neuroscience.2016.02.037
- Bushnell, B. (2014). *BBMap: a fast, accurate, splice-aware aligner*. Available at: <https://www.osti.gov/biblio/1241166>.
- Chao, B., Zhang, L., Pan, J., Zhang, Y., Chen, Y., Xu, M., et al. (2021). Stanniocalcin-1 overexpression prevents depression-like behaviors through inhibition of the ROS/NF-κB signaling pathway. *Psychiatry* 12, 644383. doi:10.3389/fpsy.2021.644383
- Charlton, R., Jordan, S., Pierini, A., Garne, E., Neville, A., Hansen, A., et al. (2015). Selective serotonin reuptake inhibitor prescribing before, during and after pregnancy: a population-based study in six European regions. *BJOG An Int. J. Obstetrics Gynaecol.* 122, 1010–1020. doi:10.1111/1471-0528.13143
- Chen, D., Yu, W., Aitken, L., and Gunn-Moore, F. (2021). Willin/FRMD6: a multi-functional neuronal protein associated with alzheimer's disease. *Cells* 10, 3024. doi:10.3390/cells10113024
- Chen, Y., Meng, J., Bi, F., Li, H., Chang, C., Ji, C., et al. (2019). EK7 regulates NLRP3 inflammasome activation and neuroinflammation post-traumatic brain injury. *Front. Mol. Neurosci.* 12, 202. doi:10.3389/fnmol.2019.00202
- Chen, Y. A., Lemire, M., Choufani, S., Butcher, D. T., Grafodatskaya, D., Zanke, B. W., et al. (2013). Discovery of cross-reactive probes and polymorphic CpGs in the Illumina Infinium HumanMethylation450 microarray. *Epigenetics* 8, 203–209. doi:10.4161/epi.23470
- Chergui, K., Svenningsson, P., and Greengard, P. (2005). Physiological role for casein kinase 1 in glutamatergic synaptic transmission. *J. Neurosci.* 25, 6601–6609. doi:10.1523/jneurosci.1082-05.2005
- Clifford, M. A., Athar, W., Leonard, C. E., Russo, A., Sampognaro, P. J., Goes, M. S. V. D., et al. (2014). EphA7 signaling guides cortical dendritic development and spine maturation. *Proc. Natl. Acad. Sci. U. S. A.* 111, 4994–4999. doi:10.1073/pnas.1323793111
- Cooper, W. O., Willy, M. E., Pont, S. J., and Ray, W. A. (2007). Increasing use of antidepressants in pregnancy. *Am. J. Obstet. Gynecol.* 196, e1–e5. doi:10.1016/j.ajog.2007.01.033
- Curzytek, K., and Leskiewicz, M. (2021). Targeting the CCL2-CCR2 axis in depressive disorders. *Pharmacol. Rep.* 73, 1052–1062. doi:10.1007/s43440-021-00280-w
- Daniel, D. C., and Johnson, E. M. (2018). PURA, the gene encoding Pur-alpha, member of an ancient nucleic acid-binding protein family with mammalian neurological functions. *Gene* 643, 133–143. doi:10.1016/j.gene.2017.12.004
- Ehler, E., van Leeuwen, F., Collard, J. G., and Salinas, P. C. (1997). Expression of Tiam-1 in the developing brain suggests a role for the tiam-1–rac signaling pathway in cell migration and neurite outgrowth. *Mol. Cell. Neurosci.* 9, 1–12. doi:10.1006/mcne.1997.0602
- Feng, W., Shao, C., and Liu, H.-K. (2017). Versatile roles of the chromatin remodeler CHD7 during brain development and disease. *Front. Mol. Neurosci.* 10, 309. doi:10.3389/fnmol.2017.00309
- Fortin, J. P., Labbe, A., Lemire, M., Zanke, B. W., Hudson, T. J., Fertig, E. J., et al. (2014). Functional normalization of 450k methylation array data improves replication in large cancer studies. *Genome Biol.* 15, 503. doi:10.1186/s13059-014-0503-2
- Gerges, P., Bitar, T., Laumonier, F., Marouillat, S., Nemer, G., Andres, C. R., et al. (2022). Identification of novel gene variants for autism spectrum disorders in the Lebanese population using whole-exome sequencing. *Genes* 13, 186. doi:10.3390/genes13020186
- Gui, S. W., Liu, Y. Y., Zhong, X. G., Liu, X., Zheng, P., Pu, J. C., et al. (2018). Plasma disturbance of phospholipid metabolism in major depressive disorder by integration of proteomics and metabolomics. *Neuropsychiatric Dis. Treat.* 14, 1451–1461. doi:10.2147/ndt.s164134
- Hafemeister, C., and Satija, R. (2019). Normalization and variance stabilization of single-cell RNA-seq data using regularized negative binomial regression. *bioRxiv*, 576827. doi:10.1101/576827
- Han, K.-M., Han, M.-R., Kim, A., Kang, W., Kang, Y., Kang, J., et al. (2020). A study combining whole-exome sequencing and structural neuroimaging analysis for major depressive disorder. *J. Affect. Disord.* 262, 31–39. doi:10.1016/j.jad.2019.10.039
- Hanley, G. E., Brain, U., and Oberlander, T. F. (2015). Prenatal exposure to serotonin reuptake inhibitor antidepressants and childhood behavior. *Pediatr. Res.* 78, 174–180. doi:10.1038/pr.2015.77
- Hao, Y., Stuart, T., Kowalski, M. H., Choudhary, S., Hoffman, P., Hartman, A., et al. (2024). Dictionary learning for integrative, multimodal and scalable single-cell analysis. *Nat. Biotechnol.* 42, 293–304. doi:10.1038/s41587-023-01767-y
- Hastie, T. (2022). *Gam: generalized additive models*. Available at: <https://cran.r-project.org/package=gam>.
- Hendrick, V., Stowe, Z. N., Altshuler, L. L., Hwang, S., Lee, E., and Haynes, D. (2003). Placental passage of antidepressant medications. *Am. J. Psychiatry* 160, 993–996. doi:10.1176/appi.ajp.160.5.993
- Hiemke, C., Bergemann, N., Clement, H. W., Conca, A., Deckert, J., Domschke, K., et al. (2018). Consensus guidelines for therapeutic drug monitoring in neuropsychopharmacology: update 2017. *Pharmacopsychiatry* 51, 9–62. doi:10.1055/s-0043-116492
- Hiew, L.-F., Poon, C.-H., You, H.-Z., and Lim, L.-W. (2021). TGF-β/Smad signalling in neurogenesis: implications for neuropsychiatric diseases. *Cells* 10, 1382. doi:10.3390/cells10061382
- Hjorth, S., Bromley, R., Ystrom, E., Lupattelli, A., Spigset, O., and Nordeng, H. (2019). Use and validity of child neurodevelopment outcome measures in studies on prenatal exposure to psychotropic and analgesic medications – a systematic review. *PLOS ONE* 14, e0219778. doi:10.1371/journal.pone.0219778
- Hyde, C. L., Nagle, M. W., Tian, C., Chen, X., Paciga, S. A., Wendland, J. R., et al. (2016). Identification of 15 genetic loci associated with risk of major depression in individuals of European descent. *Nat. Genet.* 48, 1031–1036. doi:10.1038/ng.3623
- Ichinose, M., Suzuki, N., Wang, T., Kobayashi, H., Vrbancak, L., Ng, J. Q., et al. (2021). The BMP antagonist Gremlin1 contributes to the development of cortical excitatory neurons, motor balance and fear responses. *Development* 148, dev195883. doi:10.1242/dev.195883
- Jiang, H. Y., Peng, C. T., Zhang, X., and Ruan, B. (2018). Antidepressant use during pregnancy and the risk of attention-deficit/hyperactivity disorder in the children: a meta-analysis of cohort studies. *BJOG An Int. J. Obstetrics Gynaecol.* 125, 1077–1084. doi:10.1111/1471-0528.15059
- Jimenez-Solem, E., Andersen, J. T., Petersen, M., Broedbaek, K., Andersen, N. L., Torp-Pedersen, C., et al. (2013). Prevalence of antidepressant use during pregnancy in Denmark, a nation-wide cohort study. *PLoS ONE* 8, e63034. doi:10.1371/journal.pone.0063034
- Kaddurah-Daouk, R., Bogdanov, M. B., Wikoff, W. R., Zhu, H., Boyle, S. H., Churchill, E., et al. (2013). Pharmacometabolomic mapping of early biochemical changes induced by sertraline and placebo. *Transl. Psychiatry* 3, e223. doi:10.1038/tp.2012.142
- Karachaliou, C.-E., and Livanou, E. (2023). Neuroprotective action of humanin and humanin analogues: research findings and perspectives. *Biology* 12, 1534. doi:10.3390/biology12121534
- Kassambara, A. (2020). *Ggpubr: “ggplot2” based publication ready plots*.
- Kim, D., Langmead, B., and Salzberg, S. L. (2015). HISAT: a fast spliced aligner with low memory requirements. *Nat. Methods* 12, 357–360. doi:10.1038/nmeth.3317
- Klinger, G., Frankenthal, D., Merlob, P., Diamond, G., Sirota, L., Levinson-Castiel, R., et al. (2011). Long-term outcome following selective serotonin reuptake inhibitor induced neonatal abstinence syndrome. *J. Perinatology* 31, 615–620. doi:10.1038/jp.2010.211
- Kobayashi, T., Matsuyama, T., Takeuchi, M., and Ito, S. (2016). Autism spectrum disorder and prenatal exposure to selective serotonin reuptake inhibitors: a systematic review and meta-analysis. *Reprod. Toxicol.* 65, 170–178. doi:10.1016/j.reprotox.2016.07.016
- Kolde, R. (2019). *Pheatmap: pretty heatmaps*.
- Kuehner, J. N., Walia, N. R., Seong, R., Li, Y., Martinez-Feduchi, P., and Yao, B. (2023). Social defeat stress induces genome-wide 5mC and 5hmC alterations in the mouse brain. *G3 Genes, Genomes, Genet.* 13, jkad114. doi:10.1093/g3journal/jkad114

- Kundakovic, M., and Jaric, I. (2017). The epigenetic link between prenatal adverse environments and neurodevelopmental disorders. *Genes* 2017, Vol. 8, Page 104 (8), 104. doi:10.3390/genes8030104
- Kunde, S., Rademacher, N., Zieger, H., and Shoichet, S. A. (2017). Protein kinase C regulates AMPA receptor auxiliary protein Shisa9/CKAMP44 through interactions with neuronal scaffold PICK1. *FEBS Open Bio* 7, 1234–1245. doi:10.1002/2211-5463.12261
- LaManno, G., Gyllborg, D., Codeluppi, S., Nishimura, K., Salto, C., Zeisel, A., et al. (2016). Molecular diversity of midbrain development in mouse, human, and stem cells. *Cell* 167, 566–580. doi:10.1016/j.cell.2016.09.027
- László, Z. I., and Lele, Z. (2022). Flying under the radar: CDH2 (N-cadherin), an important hub molecule in neurodevelopmental and neurodegenerative diseases. *Front. Neurosci.* 16, 972059. doi:10.3389/fnins.2022.972059
- Liao, Y., Smyth, G. K., and Shi, W. (2014). FeatureCounts: an efficient general purpose program for assigning sequence reads to genomic features. *Bioinformatics* 30, 923–930. doi:10.1093/bioinformatics/btt656
- Licht, T., Eavri, R., Goshen, I., Shlomai, Y., Mizrahi, A., and Keshet, E. (2009). VEGF is required for dendritogenesis of newly born olfactory bulb interneurons. *Development* 137, 261–271. doi:10.1242/dev.039636
- Lin, H. H., Bell, E., Uwanogho, D., Perfect, L. W., Noristani, H., Bates, T. J. D., et al. (2010). Neuronatin promotes neural lineage in ESCs via Ca²⁺ signaling. *Stem Cells Dayt. Ohio* 28, 1950–1960. doi:10.1002/stem.530
- Lu, H.-C., Tan, Q., Rousseaux, M. W. C., Wang, W., Kim, J.-Y., Richman, R., et al. (2017). Disruption of the ATXN1–CIC complex causes a spectrum of neurobehavioral phenotypes in mice and humans. *Nat. Genet.* 49, 527–536. doi:10.1038/ng.3808
- Ludden, T. M. (1991). Nonlinear pharmacokinetics: clinical Implications. *Clin. Pharmacokinet.* 20, 429–446. doi:10.2165/00003088-199120060-00001
- Lun, A. T. L., Chen, Y., and Smyth, G. K. (2016). It's DE-licious: a recipe for differential expression analyses of RNA-seq experiments using quasi-likelihood methods in edgeR. *Methods Mol. Biol.* 1418, 391–416. doi:10.1007/978-1-4939-3578-9_19
- Lupatelli, A., Wood, M., Ystrom, E., Skurtveit, S., Handal, M., and Nordeng, H. (2018). Effect of time-dependent selective serotonin reuptake inhibitor antidepressants during pregnancy on behavioral, emotional, and social development in preschool-aged children. *J. Am. Acad. Child Adolesc. Psychiatry* 57, 200–208. doi:10.1016/j.jaac.2017.12.010
- MacQueen, G., and Frodl, T. (2010). The hippocampus in major depression: evidence for the convergence of the bench and bedside in psychiatric research? *Mol. Psychiatry* 2011 16:3 16, 252–264. doi:10.1038/mp.2010.80
- MahmoudianDehkordi, S., Ahmed, A. T., Bhattacharyya, S., Han, X., Baillie, R. A., Arnold, M., et al. (2021). Alterations in acylcarnitines, amines, and lipids inform about the mechanism of action of citalopram/escitalopram in major depression. *Transl. Psychiatry* 2021 11:1 11, 153–214. doi:10.1038/s41398-020-01097-6
- Main, H., Hedenskog, M., Acharya, G., Hovatta, O., and Lanner, F. (2020). Karolinska Institutet human embryonic stem cell bank. *Stem Cell Res.* 45, 101810. doi:10.1016/j.scr.2020.101810
- Malberg, J. E., Eisch, A. J., Nestler, E. J., and Duman, R. S. (2000). Chronic antidepressant treatment increases neurogenesis in adult rat Hippocampus. *J. Neurosci.* 20, 9104–9110. doi:10.1523/jneurosci.20-24-09104.2000
- Mallick, A., Sharma, M., and Dey, C. S. (2022). Emerging roles of PHLPP phosphatases in the nervous system. *Mol. Cell. Neurosci.* 123, 103789. doi:10.1016/j.mcn.2022.103789
- Malm, H., Brown, A. S., Gissler, M., Gyllenberg, D., Hinkka-Yli-Salomäki, S., McKeague, I. W., et al. (2016). Gestational exposure to selective serotonin reuptake inhibitors and offspring psychiatric disorders: a national register-based study. *J. Am. Acad. Child Adolesc. Psychiatry* 55, 359–366. doi:10.1016/j.jaac.2016.02.013
- Manning, C. S., Biga, V., Boyd, J., Kursawe, J., Ymison, B., Spiller, D. G., et al. (2019). Quantitative single-cell live imaging links HES5 dynamics with cell-state and fate in murine neurogenesis. *Nat. Commun.* 2019 10:1 10, 2835–2919. doi:10.1038/s41467-019-10734-8
- Marziali, F., Dizanzo, M. P., Cavatorta, A. L., and Gardiol, D. (2019). Differential expression of DLG1 as a common trait in different human diseases: an encouraging issue in molecular pathology. *Biol. Chem.* 400, 699–710. doi:10.1515/hsz-2018-0350
- Mateus-Pinheiro, A., Pinto, L., Bessa, J. M., Morais, M., Alves, N. D., Monteiro, S., et al. (2013). Sustained remission from depressive-like behavior depends on hippocampal neurogenesis. *Transl. Psychiatry* 2013 3:1 3, e210. doi:10.1038/tp.2012.141
- McCarthy, D. J., Campbell, K. R., Lun, A. T. L., and Wills, Q. F. (2017). Scater: pre-processing, quality control, normalization and visualization of single-cell RNA-seq data in R. *Bioinformatics* 33, 1179–1186. doi:10.1093/bioinformatics/btw777
- Meyers, E. A., and Kessler, J. A. (2017). TGF- β family signaling in neural and neuronal differentiation, development, and function. *Cold Spring Harb. Perspect. Biol.* 9, a022244. doi:10.1101/cshperspect.a022244
- Mitchell, A. A., Gilboa, S. M., Werler, M. M., Kelley, K. E., Louik, C., Hernández-Díaz, S., et al. (2011). Medication use during pregnancy, with particular focus on prescription drugs: 1976–2008. *Am. J. Obstet. Gynecol.* 205, 51.e1–51.e18. doi:10.1016/j.ajog.2011.02.029
- Mitsiadis, T. A., Pagella, P., and Cantù, C. (2017). Early determination of the periodontal domain by the Wnt-Antagonist Frzb/Sfrp3. *Front. Physiology* 8, 936. doi:10.3389/fphys.2017.00936
- Moigneu, C., Abdellaoui, S., Ramos-Brossier, M., Pfaffenseller, B., Wollenhaupt-Aguiar, B., Cardoso, T., et al. (2023). Systemic GDF11 attenuates depression-like phenotype in aged mice via stimulation of neuronal autophagy. *Nat. Aging* 2023 3:2 3, 213–228. doi:10.1038/s43587-022-00352-3
- Molitor, L., Bacher, S., Burczyk, S., and Niessing, D. (2021). The molecular function of PURA and its implications in neurological diseases. *Front. Genet.* 12, 638217. doi:10.3389/fgene.2021.638217
- Moore, K. L., Persaud, T. V. N., and Torchia, M. G. (2016). *The developing human—clinically oriented embryology*. 10th Edn. Philadelphia, PA: Saunders Elsevier. Available at: https://www.academia.edu/44502808/The_Developing_Human_Clinically_Oriented_Embryology_by_Keith_L_Moore (Accessed June 29, 2023).
- Morales, D. R., Slattery, J., Evans, S., and Kurz, X. (2018). Antidepressant use during pregnancy and risk of autism spectrum disorder and attention deficit hyperactivity disorder: systematic review of observational studies and methodological considerations. *BMC Med.* 16, 6–14. doi:10.1186/s12916-017-0993-3
- Nautiyal, K. M., and Hen, R. (2017). Serotonin receptors in depression: from A to B. *Front. Neurosci.* 11, 1268881. doi:10.3389/fnins.2017.0126881
- Nordeng, H., Gelder, M. M. H. J. V., Spigset, O., Koren, G., Einarson, A., and Eberhard-Gran, M. (2012). Pregnancy outcome after exposure to antidepressants and the role of maternal depression: results from the Norwegian mother and child cohort study. *J. Clin. Psychopharmacol.* 32, 186–194. doi:10.1097/jcp.0b013e3182490eaf
- Oh, W. J., and Gu, C. (2013). The role and mechanism-of-action of Sema3E and Plexin-D1 in vascular and neural development. *Seminars Cell and Dev. Biol.* 24, 156–162. doi:10.1016/j.semcdb.2012.12.001
- Olstad, E. W., Marie, H., Nordeng, E., Sandve, G. K., Lyle, R., and Gervin, K. (2023). Effects of prenatal exposure to (es)citalopram and maternal depression during pregnancy on DNA methylation and child neurodevelopment. *Transl. Psychiatry* 13, 149–211. doi:10.1038/s41398-023-02441-2
- Oyang, E. L., Davidson, B. C., Lee, W., and Poon, M. M. (2011). Functional characterization of the dendritically localized mRNA neuronatin in hippocampal neurons. *PLoS ONE* 6, e24879. doi:10.1371/journal.pone.0024879
- Oyola, M. G., and Handa, R. J. (2017). Hypothalamic–pituitary–adrenal and hypothalamic–pituitary–gonadal axes: sex differences in regulation of stress responsivity. *Stress* 20, 476–494. doi:10.1080/10253890.2017.1369523
- Pan, Z. Z. (2012). Transcriptional control of Gad2. *Transcription* 3, 68–72. doi:10.4161/trns.19511
- Paoletti, P., Bellone, C., and Zhou, Q. (2013). NMDA receptor subunit diversity: impact on receptor properties, synaptic plasticity and disease. *Nat. Rev. Neurosci.* 2013 14:6 14, 383–400. doi:10.1038/nrn3504
- Paulzen, M., Goecke, T. W., Stingl, J. C., Janssen, G., Stickeler, E., Gründer, G., et al. (2017). Pregnancy exposure to citalopram – therapeutic drug monitoring in maternal blood, amniotic fluid and cord blood. *Prog. Neuro-Psychopharmacology Biol. Psychiatry* 79, 213–219. doi:10.1016/j.pnpbp.2017.06.030
- Perera, T. D., Dwork, A. J., Keegan, K. A., Thirumangalakudi, L., Lipira, C. M., Joyce, N., et al. (2011). Necessity of hippocampal neurogenesis for the therapeutic action of antidepressants in adult nonhuman primates. *PLOS ONE* 6, e17600. doi:10.1371/journal.pone.0017600
- Phipson, B., Maksimovic, J., and Oshlack, A. (2016). MissMethyl: an R package for analyzing data from Illumina's HumanMethylation450 platform. *Bioinformatics* 32, 286–288. doi:10.1093/bioinformatics/btv560
- Pollock, B. G. (2001). Citalopram: a comprehensive review. *Expert Opin. Pharmacother.* 2, 681–698. doi:10.1517/14656566.2.4.681
- Porter, G. A., and O'Connor, J. C. (2022). Brain-derived neurotrophic factor and inflammation in depression: pathogenic partners in crime? *World J. Psychiatry* 12, 77–97. doi:10.5498/wjpv.12.1.77
- R Core Team (2021). *R: a language and environment for statistical computing*. Vienna, Austria. Available at: <https://www.r-project.org/>.
- Rampono, J., Simmer, K., Ilett, K. F., Hackett, L. P., Doherty, D. A., Elliot, R., et al. (2009). Placental transfer of SSRI and SNRI antidepressants and effects on the neonate. *Pharmacopsychiatry* 42, 95–100. doi:10.1055/s-0028-1103296
- Ramsteijn, A. S., de Wijer, L. V., Rando, J., van Luijk, J., Homberg, J. R., and Olivier, J. D. A. (2020). Perinatal selective serotonin reuptake inhibitor exposure and behavioral outcomes: a systematic review and meta-analysis of animal studies. *Neurosci. Biobehav. Rev.* 114, 53–69. doi:10.1016/j.neubiorev.2020.04.010
- Ribeiro, S., and Sherrard, R. M. (2023). Cerebellum and neurodevelopmental disorders: ROR α is a unifying force. *Front. Cell. Neurosci.* 17, 1108339. doi:10.3389/fncel.2023.1108339
- Riggs, E., Shakkour, Z., Anderson, C. L., and Carney, P. R. (2022). SYT1-Associated neurodevelopmental disorder: a narrative review. *Children* 9, 1439. doi:10.3390/children9101439
- Ritchie, M. E., Phipson, B., Wu, D., Hu, Y., Law, C. W., Shi, W., et al. (2015). Limma powers differential expression analyses for RNA-sequencing and microarray studies. *Nucleic Acids Res.* 43, e47. doi:10.1093/nar/gkv007

- Robinson, M. D., McCarthy, D. J., and Smyth, G. K. (2010). edgeR: a Bioconductor package for differential expression analysis of digital gene expression data. *Bioinformatics* 26, 139–140. doi:10.1093/bioinformatics/btp616
- Rojas-Charry, L., Nardi, L., Methner, A., and Schmeisser, M. J. (2021). Abnormalities of synaptic mitochondria in autism spectrum disorder and related neurodevelopmental disorders. *J. Mol. Med.* 99, 161–178. doi:10.1007/s00109-020-02018-2
- Samara, A., Falck, M., Spildrejorde, M., Leithaug, M., Acharya, G., Lyle, R., et al. (2022a). Robust neuronal differentiation of human embryonic stem cells for neurotoxicology. *Star. Protoc.* 3, 101533. doi:10.1016/j.xpro.2022.101533
- Samara, A., Spildrejorde, M., Sharma, A., Gervin, K., Lyle, R., Eskeland, R., et al. (2022b). A multi-omics approach to visualize early neuronal differentiation from hESCs in 4D. *iScience* 25, 105279. doi:10.1016/j.isci.2022.105279
- Sanders, S. S., Hernandez, L. M., Soh, H., Karnam, S., Walikonis, R. S., Tzingounis, A. V., et al. (2020). The palmitoyl acyltransferase ZDHHC14 controls Kv1-family potassium channel clustering at the axon initial segment. *eLife* 9, 560588–e56132. doi:10.7554/eLife.56058
- Sangkuhl, K., Klein, T. E., and Altman, R. B. (2011). PharmGKB summary: citalopram pharmacokinetics pathway. *Pharmacogenet. Genom.* 21, 769–772. doi:10.1097/fpc.0b013e328346063f
- Saveanu, R. V., and Nemeroff, C. B. (2012). Etiology of depression: genetic and environmental factors. *PSC* 35, 51–71. doi:10.1016/j.psc.2011.12.001
- Shi, Y., and Liu, J.-P. (2011). Gdf11 facilitates temporal progression of neurogenesis in the developing spinal cord. *J. Neurosci.* 31, 883–893. doi:10.1523/jneurosci.2394-10.2011
- Sirignano, L., Frank, J., Kranaster, L., Witt, S. H., Streit, F., Zillich, L., et al. (2021). Methylome-wide change associated with response to electroconvulsive therapy in depressed patients. *Transl. Psychiatry* 11, 347. doi:10.1038/s41398-021-01474-9
- Song, Y., Cao, H., Zuo, C., Gu, Z., Huang, Y., Miao, J., et al. (2023). Mitochondrial dysfunction: a fatal blow in depression. *Biomed. Pharmacother.* 167, 115652. doi:10.1016/j.biopha.2023.115652
- Spildrejorde, M., Samara, A., Sharma, A., Leithaug, M., Falck, M., Modafferi, S., et al. (2023). Multi-omics approach reveals dysregulated genes during hESCs neuronal differentiation exposure to paracetamol. *iScience* 26 (10), 107755. doi:10.1016/j.isci.2023.107755
- Street, K., Rizzo, D., Fletcher, R. B., Das, D., Ngai, J., Yosef, N., et al. (2018). Slingshot: cell lineage and pseudotime inference for single-cell transcriptomics. *BMC Genomics* 19, 477–516. doi:10.1186/s12864-018-4772-0
- Ström, S., Holm, F., Bergström, R., Strömberg, A. M., and Hovatta, O. (2010). Derivation of 30 human embryonic stem cell lines—improving the quality. *Vitro Cell. Dev. Biol. Animal* 46, 337–344. doi:10.1007/s11626-010-9308-0
- Stuart, T., Butler, A., Hoffman, P., Hafemeister, C., Papalexi, E., Mauck, W. M., et al. (2019). Comprehensive integration of single-cell data. *Cell* 177, 1888–1902. doi:10.1016/j.cell.2019.05.031
- Subramanian, A., Tamayo, P., Mootha, V. K., Mukherjee, S., Ebert, B. L., Gillette, M. A., et al. (2005). Gene set enrichment analysis: a knowledge-based approach for interpreting genome-wide expression profiles. *Proc. Natl. Acad. Sci.* 102, 15545–15550. doi:10.1073/pnas.0506580102
- Tate, K., Kirk, B., Tseng, A., Ulfers, A., and Litwa, K. (2021). Effects of the selective serotonin reuptake inhibitor fluoxetine on developing neural circuits in a model of the human fetal cortex. *Int. J. Mol. Sci.* 22, 10457. doi:10.3390/ijms221910457
- Tian, Y., Milic, J., Monasor, L. S., Chakraborty, R., Wang, S., Yuan, Y., et al. (2023). The COP9 signalosome reduces neuroinflammation and attenuates ischemic neuronal stress in organotypic brain slice culture model. *Cell. Mol. Life Sci.* 80, 262. doi:10.1007/s00018-023-04911-8
- Tirosh, I., Izar, B., Prakadan, S. M., Wadsworth, M. H., Treacy, D., Trombetta, J. J., et al. (2016). Dissecting the multicellular ecosystem of metastatic melanoma by single-cell RNA-seq. *Science* 352, 189–196. doi:10.1126/science.aad0501
- Tirozzi, A., Quiccione, M. S., Cerletti, C., Donati, M. B., Gaetano, G., Iacoviello, L., et al. (2023). A multi-trait association analysis of brain disorders and platelet traits identifies novel susceptibility loci for major depression, alzheimer's and Parkinson's disease. *Cells* 12, 245. doi:10.3390/cells12020245
- Tocco, C., Bertacchi, M., and Studer, M. (2021). Structural and functional aspects of the neurodevelopmental gene NR2F1: from animal models to human pathology. *Front. Mol. Neurosci.* 14, 767965. doi:10.3389/fnmol.2021.767965
- Triche, T. J., Weisenberger, D. J., Berg, D. V. D., Laird, P. W., and Siegmund, K. D. (2013). Low-level processing of Illumina Infinium DNA methylation BeadArrays. *Nucleic Acids Res.* 41, e90. doi:10.1093/nar/gkt090
- Unschuld, P. G., Ising, M., Specht, M., Erhardt, A., Ripke, S., Heck, A., et al. (2009). Polymorphisms in the GAD2 gene-region are associated with susceptibility for unipolar depression and with a risk factor for anxiety disorders. *Am. J. Med. Genet. Part B Neuropsychiatric Genet.* 150B, 1100–1109. doi:10.1002/ajmg.b.30938
- Vance, K. W., Sansom, S. N., Lee, S., Chalei, V., Kong, L., Cooper, S. E., et al. (2014). The long non-coding RNA Paupar regulates the expression of both local and distal genes. *EMBO J.* 33, 296–311. doi:10.1002/emboj.201386225
- Wagner, N. R., and MacDonald, J. L. (2021). Atypical neocortical development in the Cited2 conditional knockout leads to behavioral deficits associated with neurodevelopmental disorders. *Neuroscience* 455, 65–78. doi:10.1016/j.neuroscience.2020.12.009
- Wang, L., Zhang, J., Li, G., Cao, C., Fang, R., Liu, P., et al. (2021). The ADCYAP1R1 gene is correlated with posttraumatic stress disorder symptoms through diverse epistases in a traumatized Chinese population. *Front. Psychiatry* 12, 665599. doi:10.3389/fpsy.2021.665599
- Wang, Q., Zhao, G., Yang, Z., Liu, X., and Xie, P. (2018). Downregulation of microRNA-124-3p suppresses the mTOR signaling pathway by targeting DDIT4 in males with major depressive disorder. *Int. J. Mol. Med.* 41, 493–500. doi:10.3892/ijmm.2017.3235
- Wickham, H., Averick, M., Bryan, J., Chang, W., McGowan, L., François, R., et al. (2019). Welcome to the Tidyverse. *J. Open Source Softw.* 4, 1686. doi:10.21105/joss.01686
- Witte, L. D., Wang, Z., Snijders, G. L. J. L., Mendelev, N., Liu, Q., Sneebouer, M. A. M., et al. (2022). Contribution of age, brain region, mood disorder pathology, and interindividual factors on the methylome of human microglia. *Biol. Psychiatry* 91, 572–581. doi:10.1016/j.biopsych.2021.10.020
- Woo, H.-I., Chun, M.-R., Yang, J.-S., Lim, S.-W., Kim, M.-J., Kim, S.-W., et al. (2015). Plasma amino acid profiling in major depressive disorder treated with selective serotonin reuptake inhibitors. *CNS Neurosci. Ther.* 21 (5), 417–424. doi:10.1111/cns.12372
- Xu, J., Xia, X., Li, Q., Dou, Y., Suo, X., Sun, Z., et al. (2022). A causal association of ANKRD37 with human hippocampal volume. *Mol. Psychiatry* 27, 4432–4445. doi:10.1038/s41380-022-01800-7
- Yang, Y., Zhou, X., Liu, X., Song, R., Gao, Y., and Wang, S. (2021). Implications of FBXW7 in neurodevelopment and neurodegeneration: molecular mechanisms and therapeutic potential. *Front. Cell. Neurosci.* 15, 736008. doi:10.3389/fncel.2021.736008
- Zappia, L., and Oshlack, A. (2018). Clustering trees: a visualization for evaluating clusterings at multiple resolutions. *GigaScience* 7, giy083. doi:10.1093/gigascience/giy083
- Zhang, Z., and Zhao, Y. (2022). Progress on the roles of MEF2C in neuropsychiatric diseases. *Mol. Brain* 15, 8. doi:10.1186/s13041-021-00892-6
- Zhong, X., Harris, G., Smirnova, L., Zufferey, V., Sá, R., Russo, F. B., et al. (2020). Antidepressant paroxetine exerts developmental neurotoxicity in an iPSC-derived 3D human brain model. *Front. Cell. Neurosci.* 14, 25. doi:10.3389/fncel.2020.00025
- Zhou, X., Lindsay, H., and Robinson, M. D. (2014). Robustly detecting differential expression in RNA sequencing data using observation weights. *Nucleic Acids Res.* 42, e91. doi:10.1093/nar/gku310
- Ziegler, G. C., Almos, P., McNeill, R. V., Jansch, C., and Lesch, K. P. (2020). Cellular effects and clinical implications of SLC2A3 copy number variation. *J. Cell. Physiology* 235, 9021–9036. doi:10.1002/jcp.29753
- Zoega, H., Kieler, H., Nørgaard, M., Furu, K., Valdimarsdóttir, U., Brandt, L., et al. (2015). Use of SSRI and snri antidepressants during pregnancy: a population-based study from Denmark, Iceland, Norway and Sweden. *PLOS ONE* 10, e0144474. doi:10.1371/journal.pone.0144474